

WHITNEYAN (MIDDLE OLIGOCENE) RODENTS
FROM OBRITSCH RANCH (STARK COUNTY, NORTH DAKOTA)
AND A REVIEW OF WHITNEYAN RODENT FOSSIL RECORD

WILLIAM W. KORTH

[Research Associate, Section of Vertebrate Paleontology, Carnegie Museum of Natural History]
Rochester Institute of Vertebrate Paleontology,
265 Carling Road, Rochester, New York 14610
wwkorth@frontiernet.net

CLINT A. BOYD

North Dakota Geological Survey,
600 East Boulevard Ave., Bismarck, North Dakota 58505
caboyd@nd.gov

JEFF J. PERSON

North Dakota Geological Survey,
600 East Boulevard Ave., Bismarck, North Dakota 58505
jjperson@nd.gov

ABSTRACT

Until recently, few well-described rodent faunae from the Whitneyan North American Land Mammal Age [NALMA] were known, hindering studies of rodent diversity, biogeography, and evolutionary patterns during the Oligocene. This study describes a new Whitneyan rodent assemblage from the Obritsch Ranch paleontological locality in the Little Badlands region of North Dakota. Specimens were collected from three stratigraphically restricted sampling intervals within the middle to upper Brule Formation, resulting in the recognition of fourteen rodent species, five of which are elsewhere known to first appear in Whitneyan faunae. Described is one **new species**, the eomyid *Paradjidaumo obritschorum*, and the first cranial material of the heteromyid rodent *Proharymys* Korth and Branciforte, 2007. The rodent fauna from the upper two sampling intervals at Obritsch Ranch and the uppermost fauna recently described from the nearby Fitterer Ranch paleontological locality share four taxa in common with the late Whitneyan Blue Ash local fauna from southwestern South Dakota, indicating these two North Dakota rodent faunae are also from the late Whitneyan. Increasing knowledge of Whitneyan rodent faunae in North America reveals unusually high survivorship of rodent species from the older Orellan NALMA into the Whitneyan NALMA and much geographic variation in the diversity, distribution, and relative abundance of different rodent families between individual Whitneyan rodent faunae. Those factors help explain prior difficulties in differentiating Orellan and Whitneyan rodent faunae and in identifying biostratigraphically useful rodent taxa for the Whitneyan. Overall, Whitneyan rodent faunae from North America display an increase in the diversity of aplodontiids, cricetids, and sciurids and a decrease in eomyid and ischyromyid diversity relative to the Orellan.

KEY WORDS: biostratigraphy, Brule Formation, dental nomenclature, Orellan-Whitneyan boundary, systematics

INTRODUCTION

Knowledge of Whitneyan rodent diversity has lagged behind that of other late Eocene and Oligocene North American Land Mammal Ages (NALMAs), with only 14 rodent taxa identified by Korth (1994) from Whitneyan faunae compared to 48 from the preceding Orellan NALMA (33.7–32.0 ma: Prothero and Emry 2004) and 110 from the subsequent Arikareean NALMA (30.0–18.8 ma: Tedford et al. 2004). This striking difference is often attributed to the relative scarcity of Whitneyan fossils (Prothero and Emry 2004), resulting in few well-described Whitneyan rodent faunae. This lack of understanding of Whitneyan rodent diversity impedes the study of trends in rodent diversification, rates of origination and extinction, and responses to environmental and climatic changes during the late Paleogene in North America.

Progress has been made over the last decade to increase our understanding of Whitneyan rodent diversity via the detailed description of diverse Whitneyan rodent faunae from southwestern South Dakota (Korth 2010b, 2014),

western Montana (Korth and Tabrum 2017), and southwestern North Dakota (Korth et al. 2019). The efforts of the last study were focused on the Fitterer Ranch locality within the Little Badlands area of Stark County, previously identified as preserving a largely Orellan fauna (e.g., Murphy et al. 1993; Janis et al. 2008). Review of specimens collected from that area associated with precise stratigraphic data, via both surface collection and screen washing methods, revealed that the fauna from the lowermost rocks of the Brule Formation (subunits 4A to 5A of Skinner [1951]) preserve a possible transitional Orellan/Whitneyan or Whitneyan fauna, while the middle portion (subunits 5B to 5F of Skinner [1951]) preserves a clearly Whitneyan fauna based in part on the co-presence of the cricetid *Eumys brachyodus* and the castorid *Agnotocastor praetereadens* (Korth et al. 2019).

Magnetostratigraphic study of the Brule Formation at Fitterer Ranch identified a shift from reverse polarity to normal polarity within subunit 6A, with the normal polarity

persisting at least through subunit 6E (Prothero 1996). That normal magnetozone represents Chron C12n (30.6–31.0 Ma; Ogg 2012), which is entirely contained within the late Whitneyan NALMA (30.0–31.4 Ma; Prothero and Emry 2004). Thus, it is likely that the Brule Formation in the Little Badlands area of North Dakota records the transition from an early Whitneyan rodent fauna to a late Whitneyan rodent fauna. Unfortunately, at this time insufficient rodent specimens are currently available from unit 6 at Fitterer Ranch to allow the description of a rodent fauna or facilitate accurate comparisons to the faunae collected from the lower (subunits 4A to 5A) and middle (subunits 5B to 5F) portions of the Brule Formation at that location.

The Obritsch Ranch paleontological locality is an area of geographically limited but vertically extensive outcrops of the Brule Formation situated approximately five kilometers (approximately three miles) northeast of Fitterer Ranch within the Little Badlands region (Murphy et al. 1993). Surface collection of vertebrate fossils throughout the stratigraphic section at Obritsch Ranch has been ongoing since the 1980's by the North Dakota Geological Survey (Murphy et al. 1993), with most specimens collected from three discrete stratigraphic intervals (Fig. 1). The middle interval consists of a highly fossiliferous sandstone situated within the upper portion of subunit 6 of Skinner (1951), well within rocks deposited during Chron C12n (Prothero 1996). Beginning in 2016, bulk matrix was collected from that channel sandstone and screen washed for microvertebrate fossils. That work has produced a diverse rodent fauna that is distinct from those previously described from nearby Fitterer Ranch (Korth et al. 2019). Here, we present a description of the rodent assemblage from Obritsch Ranch, with particular focus on the fauna from the middle sandstone interval, compare this new fauna to previously described Whitneyan faunae from the Great Plains region of North America, and provide an updated synthesis of rodent diversity, biogeographic patterns, and evolutionary trends during the late Eocene through Oligocene in North America.

Dental Terminology.—Dental terminology generally follows that of Wood and Wilson (1936) with specialized terminology for aplodontiids (Rensberger 1975) and castorids (Stirton 1935). Maxillary teeth are designated by capital letters, lower teeth are designated by lower-case letters (e.g., M1 and m1). All measurements were taken with optical micrometer to the nearest 0.01 mm.

Abbreviations.—Abbreviations for measurements: L, maximum anteroposterior length; W, maximum transverse width. Abbreviations for institutions: FAM, Frick Collections, American Museum of Natural History; MCZ, Museum of Comparative Zoology, Harvard University; NDGS, North Dakota State Fossil Collection, North Dakota Geological Survey; USNM PAL, US National Museum of Natural History, Smithsonian Institution.

GEOLOGIC SETTING

The Obritsch Ranch paleontological locality is situated along the southern boundary of the area commonly referred to as the Little Badlands, southwest of the city of Dickinson in Stark County, North Dakota (T138N, R97W, sections 28–29). It is situated 1.6 km east and 4.8 km north of the Fitterer Ranch paleontological locality. There are few published reviews of the geology of the rock exposures at Obritsch Ranch. Three formations are recognized at this location: the basal Chadron Formation, the middle Brule Formation, and the overlying Arikaree Formation (Stone 1973; Murphy et al. 1993). Fossils are noted from all three formations at Obritsch Ranch (Murphy et al. 1993: fig. 34), but only the rocks of the Brule Formation preserve sufficient material to permit a detailed study of the rodent assemblage at this time. At the main study location, only the Brule Formation is exposed, and neither the upper or lower contacts are present (Fig. 1).

Only the distinctive “Antelope Creek tuff” was previously identified as a useful marker bed for correlating the rocks of the Brule Formation at Fitterer Ranch and Obritsch Ranch (Murphy et al. 1993). Correlation of green to gray channel sandstones present in both areas was proposed by some authors (e.g., Stone 1973); however, multiple discontinuous channel sandstones are present at both Fitterer Ranch and Obritsch Ranch at different stratigraphic positions, most of which were deposited by localized ribbon channels, making them poor candidates for marker beds (Murphy et al. 1993). Stone (1973) proposed subdividing the Brule Formation into two informal members: the lower “Dickinson Member,” and the upper “Scheffield Member.” The transition between those informal members was placed at the base of a thick set of alternating sandstone and mudstone beds (subunit 6A of Skinner [1951], also referred to as the ‘first bedded interval’) that creates a distinct slope change in the outcrop. Though Murphy et al. (1993) decided against formalizing those members because they were difficult to differentiate elsewhere in North Dakota outside of the Little Badlands area, that bedded interval is easily traceable between Fitterer Ranch and Obritsch Ranch, assisting with stratigraphic correlations between the two areas.

Though far fewer fossils are known from Obritsch Ranch compared to Fitterer Ranch, both in terms of the number of fossiliferous horizons and total specimens collected, study of the rodent specimens from Obritsch Ranch was deemed important because many of the rodent fossils collected at Obritsch Ranch come from higher stratigraphic intervals than those previously reported from Fitterer Ranch, which were largely confined to the lower half of the Brule Formation (Korth et al. 2019). Thus, the rodent assemblage from Obritsch Ranch detailed in this study serves as a supplement to the previous work on the rodent assemblage of the Brule Formation at Fitterer Ranch, adding to our understanding of faunal distribution and turnover within the Brule Formation in North Dakota and improving regional correlations of contemporaneous rock units.

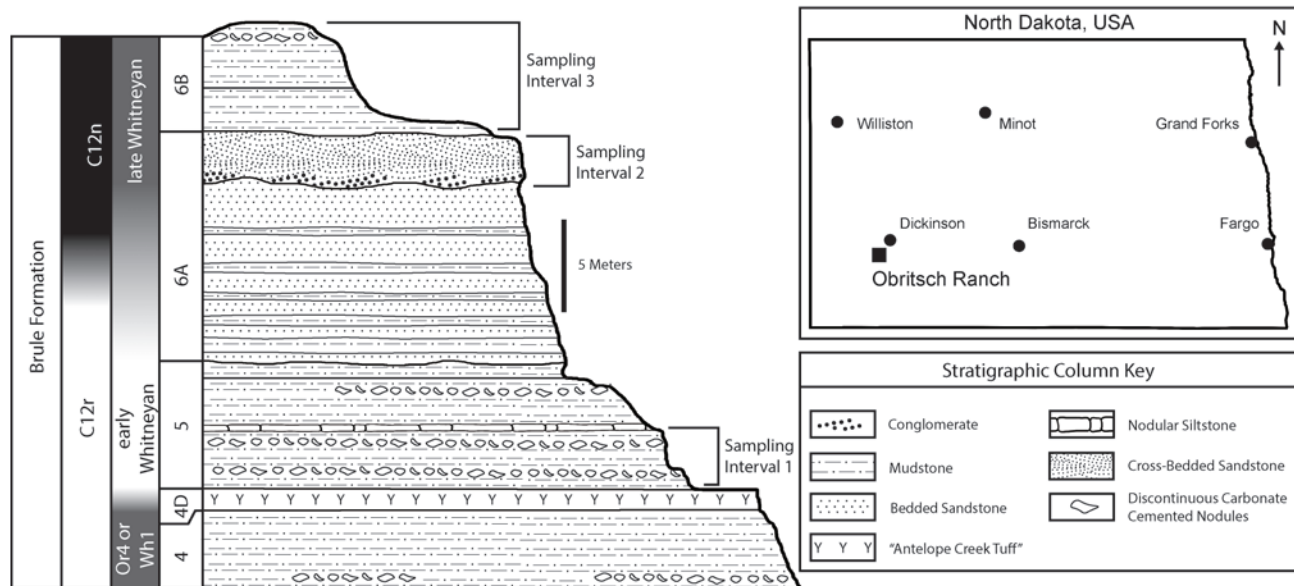


Fig. 1.—Stratigraphic section of the Brule Formation rocks exposed in the study area of Obritsch Ranch, Stark County, North Dakota. Stratigraphic data collected in 2018. Magnetostratigraphic data and rock unit numbers are based on correlations with the rocks at nearby Fitterer Ranch (Skinner 1951; Prothero 1996), and the stratigraphic distribution of mammalian faunae is based on interpretations from this study and prior work at Fitterer Ranch (Korth et al. 2019). Gradational shading for the magnetostratigraphic and biostratigraphic data reflects general uncertainty in each of those datasets. Abbreviations: C, Chron; n, normal polarity; Or4, latest Orellan NALMA; r, reverse polarity; Wh1, early Whitneyan NALMA.

SAMPLING METHODS

In this study, fossils were recovered from three distinct stratigraphic intervals (Fig. 1). This contrasts with the seven sampling intervals that were identified at nearby Fitterer Ranch where the higher abundance of fossils and more extensively exposed outcrops allowed the stratigraphic column to be subdivided more finely (Korth et al. 2019). It should be noted that these sampling intervals were defined based on ease of recognition in the field and ability to collect from rocks of one sampling interval with minimal risk of contamination by fossils of the other sampling intervals and do not necessarily correspond to lithosomes or discrete sedimentary packages in all cases. All rodent specimens collected from these intervals were identified and the resulting rodent faunae from each sampling interval were compared to assess any patterns of faunal change through time in the study area. Comparisons were also made to the rodent faunae previously reported from nearby Fitterer Ranch and from other Whitneyan faunae from the Great Plains region of North America.

Sampling Interval 1.—The base of sampling interval 1 is placed at the top of the “Antelope Creek tuff” (sensu Murphy et al. 1993), which forms a resistant ledge in the local area and serves as a useful marker bed between the Fitterer Ranch paleontological locality and the Obritsch Ranch paleontological locality. The rocks of sampling interval 1 consist mostly of silty mudstones that contain two discrete horizons of discontinuous siltstone nodules. While fossils

seem to be scattered throughout these mudstone beds, the highest concentration appears to be present in the middle mudstone interval. All specimens from this sampling interval were surface collected. The top of this sampling interval is placed at the base of a resistant nodular siltstone layer that supports a bench in the local area and clearly represents a paleosol based on the high abundance of pedotubules.

The rocks of this sampling interval at Obritsch Ranch correspond to unit 5 of Skinner (1951) at Fitterer Ranch given that the “Antelope Creek tuff” forms the top of unit 4 in that study. However, at Obritsch Ranch there is no local equivalent of the “Fitterer Channel” (sensu Skinner 1951), so exactly which of the six subunits of unit 5 these rocks correlate with is difficult to determine. Given the lack of a clear unconformity between these rocks and the underlying “Antelope Creek tuff,” it is here considered most likely that these rocks correspond with subunit 5A of Skinner (1951), but it is possible given the fossiliferous nature of these rocks that they may correspond to the highly fossiliferous rocks of subunit 5D at Fitterer Ranch and that rocks correlative with the “Fitterer Channel” (subunit 5B) were never deposited at Obritsch Ranch.

Sampling Interval 2.—The rocks of sampling interval 2 consist entirely of green to gray sandstone layers deposited within a localized ribbon channel or stacked set of ribbon channels in some locations, one of the most distinct lithologic facies exposed at Obritsch Ranch. These sandstones vary in grain size from conglomerates to fine sand, and at



Fig. 2.—Lower dentition of *Ischyromys typus* from Obritsch Ranch, NDGS 2974, right dentary with p4-m3. Anterior is to the right.

discontinuous intervals include green to brown mudball masses. Portions of these sandstones are massive, while other areas display distinct trough crossbedding developed above basal channel lags consisting of gravel to cobble sized grains. Many of those grains within the channel lags are reworked rock fragments derived from erosion of the underlying beds. These sandstones are highly fossiliferous, most commonly containing numerous bones from rhinocerotids. Microvertebrate fossils are also abundant within these sandstones, and while the vertical weathering profile of these rocks makes surface collection of fossils difficult, screen washing methods have proven highly effective at recovering fossils from these rocks. As a result, these rocks produced the most diverse rodent fauna yet identified at Obritsch Ranch. These sandstone beds are situated above a series of interbedded mudstone and silty sandstone beds that correspond to subunit 6A of Skinner (1951) at Fitterer Ranch, which were considered the basal-most unit in the informal “Scheffield Member” of Stone (1973). In some locations at Fitterer Ranch, there are laterally discontinuous sandstone stringers in the middle to upper portion of subunit 6A that are of similar composition and stratigraphic position as these sandstone beds at Obritsch Ranch, suggesting this facies was locally pervasive at Obritsch Ranch and largely absent at Fitterer Ranch. Given the position of these sandstone beds in subunit 6A, the fauna recovered from these rocks is from a higher stratigraphic interval than that reported from sampling interval 6 at Fitterer Ranch, which was collected from subunits 5E and 5F.

Sampling Interval 3.—The base of sampling interval 3 is placed at the top of the green to gray sandstone beds of sampling interval 2. The rocks of this sampling interval consist of pinkish silty mudstone beds, with silt content (and cementation) being highest at the base of the interval and decreasing vertically through the interval. Most fossils collected from this interval were surface collected as float from an extensive bench developed at the base of the interval, though fossils do weather out from the entirety of this interval. The top of this interval is placed at a discontinuous layer of siltstone nodules present within the upper portion of these pinkish mudstones, and in the local area there are no overlying rocks present that could have contaminated this sample with fossils from a younger interval. Subunits 6B and 6C at Fitterer Ranch were described by Skinner (1951) as hard, pink siltstones capped by a zone of

concretions, matching the rocks here referred to sampling interval 3. Thus, the fauna collected from these rocks is the stratigraphically highest fauna sampled from either Fitterer Ranch or Obritsch Ranch to date.

Potential Biases.—The largest potential bias in this study that impacts comparisons between faunae from the different sampling intervals at Obritsch Ranch and comparison to those previously published from nearby Fitterer Ranch is the different collection methodologies employed at each sampling interval. Surface collection of fossilized rodent specimens tends to favor collection of more complete specimens of relatively larger taxa (e.g., ischyromyids, cricetids, castorids). Alternatively, screen washing of fossiliferous rock units tends to produce mostly isolated teeth from relatively smaller rodent taxa (e.g., heliscomyids, eomyids, florentiamyids). The ideal solution is to apply both methodologies within each sampling interval; however, this is not always possible given variations in lithology, depositional environment, cementation, and fossil abundance within each sampling interval. In this study, sampling intervals 1 and 3 were sampled exclusively via surface collection because no rocks were identified in those intervals that both contained a high abundance of microvertebrate fossils and were relatively weakly cemented. Alternatively, sampling interval 2 was sampled almost exclusively via screen washing because most of the rocks within that interval were resistant to erosion and weathered into a nearly vertical profile, resulting in any fossils that do weather out being quickly lost down slope. It is important that these sampling differences be taken into consideration when comparing the faunae recovered from each interval, as well as when making comparisons to the rodent faunae reported from different sampling intervals at Fitterer Ranch that were also subjected to different sampling intervals.

Another potential bias that must be considered when comparing both between sampling intervals at Obritsch Ranch and when comparing to the rodent faunae from Fitterer Ranch is the potential bias of different depositional environments on the recovered faunae. As noted in the Fitterer Ranch study (Korth et al. 2019), all the screen washed rocks were channel sandstones, while most of the surface collected rocks were mudstones and siltstones from the adjacent floodplains or drier, upland environments. Therefore, faunal differences between sampling intervals that were studied using different sampling methodologies could also represent environmental differences. Additionally, the erosional nature and depositional environment of channel sandstone deposits could result in specimens being reworked from older rocks or transported into the area from distant regions.

TABLE 1. Dental measurements of *Ischyromys typus* from Obritsch Ranch. Measurements in mm. Abbreviations: L, anteroposterior length; W, transverse width.

NDGS#	p4L	p4W	m1L	m1W	m2L	m2W	m3L	m3W	p4– m3
2973					4.19		4.04	3.40	
2974	4.17	3.08	4.42	3.76	4.22	3.93	4.44	3.63	17.42
2975			3.94		4.01		4.27		
2976			4.15	4.14	4.33	3.90	4.23		18.54
2977			4.19	3.93					
4049	4.15	3.73	3.73	3.33	3.92	3.82			
Mean	4.16	3.41	4.09	3.74	4.13	3.88	4.25	3.52	17.98

SYSTEMATIC PALEONTOLOGY

Order Rodentia Bowdich, 1821
Family Ischyromyidae Alston, 1876
Genus *Ischyromys* Leidy, 1856

Ischyromys typus Leidy, 1856
(Fig. 2; Table 1)

Referred Specimens.—NDGS 2974, dentary with p4–m3; NDGS 2975 and 2976, dentaries with m1–m3; NDGS 4049, dentary with p4–m2 (heavily worn); NDGS 2973, partial dentary with m2–m3; NDGS 2977, dentary fragment with m1.

Occurrence.—Sampling intervals 1 and 3.

Discussion.—The specimens referred here do not differ in dental morphology from *Ischyromys typus* samples throughout western North America. In size, the dental measurements are well within the limits of collections from other localities, but near the upper limit (Heaton 1996). The size best fits the samples from the Little Badlands of southwestern North Dakota and Slim Buttes of northwestern South Dakota (Heaton 1996: fig. 5). This is not surprising, seeing that these latter collections are among the nearest geographically to Obritsch Ranch. However, specimens from nearby Fitterer Ranch, North Dakota average slightly smaller than those from Obritsch Ranch (Korth et al. 2019: table A1).

Family Aplodontiidae Brandt, 1855
Subfamily Prosciurinae Wilson, 1949
Genus *Ninamys* Vianey-Laud, Gomes, and Marivaux, 2013

Ninamys sp., cf. *N. annectens* (Korth, 1989)
(Fig. 3; Table 2)

Campestrallomys annectens Korth, 1989
Ninamys annectens (Korth), Korth, 2019

Referred Specimens.— NDGS 2963, maxilla with P3–M2; NDGS 4051, maxilla with P3–M1; NDGS 2407 and 2411, M1 or M2; NDGS 2406, 2409, p4 (partial); NDGS 2410, 2412, m1; NDGS 2403, 2964, m2; NDGS 2408, 2475, 2498, m3.

Occurrence.—Sampling intervals 1 and 2.

Description.—P3 is circular in occlusal outline with a single central cusp (Fig. 3A). The wear facet is only on the posterior half of the apex of the cusp. P4 is similar in size to the upper molars, just slightly less wide but typically expanded anteriorly at the anterobuccal corner of the tooth (Fig. 3A). The anterocone is rounded anteriorly and flattened posteriorly. There is a minute parastyle at the posterobuccal corner of the anterocone. A narrow transverse valley separates the anterocone from the protoloph. The protoloph consists of a large paracone that is weakly rounded buccally and a smaller protoconule that is slightly transversely compressed. The paracone and protoconule are connected via a short transverse loph that connects the posterolingual corner of the former to the posterobuccal corner of the latter. The protocone is crescentic, extending nearly the entire lingual length of the tooth. A short spur extends anterolingually from the buccal center of the cusp to join the posterobuccal corner of the protoconule. There is no indication of a protocone crest. The mesostyle is small and triangular-shaped at the center of the buccal margin of the tooth, blocking the central transverse valley. The metaloph consists of the metacone and metaconule, the latter being slightly larger. The metaconule is circular in occlusal outline and the metacone shows a slight amount of flattening along the buccal side with a minute loph extending posteriorly from the posterobuccal corner of the tooth. The metacone and metaconule are attached along their anterior margins from the anterolingual edge of the metacone to the anterobuccal edge of the metaconule. The metaconule contacts the center of the posterior cingulum at the postero-central point of the cusp. The metaloph does not connect with either the protoloph or protocone. There is no

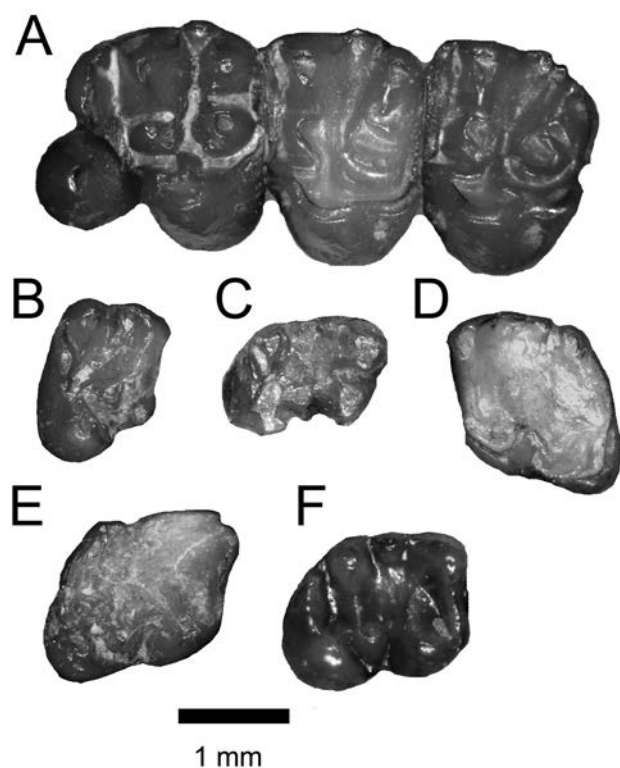


Fig. 3.—Cheek teeth of *Ninamys* sp., cf. *N. annectens* from Obritsch Ranch. **A**, NDGS 2963, maxilla with left P3–M2; **B**, NDGS 2409, right p4 (partial); **C**, NDGS 2406, right p4 (partial); **D**, NDGS 2412, left m1; **E**, NDGS 2410, right m1; **F**, NDGS 2475, right m3.

distinct hypocone, but there is a small wear facet posterior to the apex of the protocone along the posterior cingulum that runs from the posterobuccal corner of the protocone along the posterior margin of the tooth, ending at the posterobuccal extension of the metacone.

M1 lacks the anterocone of P4 (Fig. 3A). The anterior cingulum runs from the anterobuccal corner of the tooth where there is a minute parastyle along the anterior margin of the tooth and ends even with the apex of the protocone where it bends posteriorly to join the latter. There is no indication of a protocone crest on NDGS 2963, but it is present on the M1 of NDGS 4051 and there is a slight buccal bend in the cingulum anterior to the protocone in the two other referred specimens. The valley between the anterior cingulum and protoloph is thin and shallow. The cusps of the protoloph are very similar to those of P4 except that the buccal slope of the paracone is dominated by a curving loph (ectoloph) that runs from the anterobuccal corner of the paracone, then bends buccally at the apex of the cusp and bends posterobuccally, joining the anteroposteriorly elongated mesostyle at its anterior end. On NDGS 2963, there is a minute loph running posterolingually from the

posterior edge of the mesostyle that ends before reaching the metaloph. The cusps of the metaloph are as in P4. The metaconule is even larger relative to the metacone than in P4. Due to the later stage of wear, there is a minute connection between the anterolingual corner of the metacone with the lingually extending loph from the protocone. The protocone is also as in P4 with a small, distinct hypocone posterior to it.

M2 of the NDGS 2963 is virtually identical to M1 except for a slightly larger and more distinct hypocone and a minute accessory cusplule along the buccal margin, just posterior to the mesostyle (Fig. 3A). The two isolated upper molars cannot be assigned to either M1 or M2 with confidence. The only difference between these two isolated molars and those of NDGS 2963 is that there is a slight bend in the anterior arm of the protocone before it reaches the anterior cingulum, similar in position to the protocone crest, but there is no buccal extension.

Neither of the two p4s is complete. On NDGS 2409 the trigonid is complete and the metaconid and protoconid are rounded and equal in size (Fig. 3C). There is no anteroconid present, and the valley between the cusps closes posteriorly. A distinct metastylid is present on both specimens connected along the lingual margin of the tooth to the metaconid by a distinct metastylid crest. The hypoconid is the largest cusp and is obliquely oriented at the posterobuccal corner of the tooth (Fig. 3B). The ectolophid runs diagonally from the posterolingual corner of the protoconid to the anterolingual corner of the hypoconid. A distinct, rounded mesoconid is present at its center. The entoconid is anteroposteriorly compressed. The hypolophid extends buccally and slightly posteriorly from the entoconid, joining the center of the posterior cingulid where a distinct hypoconulid is present. The lingual end of the posterior cingulid does not fuse with the entoconid on the lingual side of the tooth.

Three of the four specimens of m1 or m2 are isolated, but one specimen, NDGS 2412, is retained in a fragment of the dentary and can be identified as an m1 (Fig. 3D). Because of this, the m1s can be separated from the m2s as in *N. annectens* (Korth 2019). Both molars are slightly wider than long and follow the general prosciurine pattern. The anterior width is always less than the posterior width. The metaconid is anteroposteriorly compressed and continuous with the anterior arm of the protoconid along the anterior margin of the tooth (metalophulid I). On the two specimens of m1 (NDGS 2410, NDGS 2412), the posterior arm of the protoconid extends lingually for a short distance, leaving the trigonid basin open posteriorly (Fig. 3E). On the referred m2s (NDGS 2403, NDGS 2964), the trigonid basin is closed posteriorly by the posterior arm of the protoconid (metalophulid II). However, both specimens have a greater amount of wear than the specimens of m1. On the lingual side of the tooth, the metastylid crest ends in a small mesostylid. On two of the specimens, one m1 (NDGS 2412) and one m2 (NDGS 2964), there is a second, larger mesostylid that is not continuous with the metastylid crest (Fig. 3D). The entoconid is anteroposteriorly compressed

TABLE 2. Dental measurements of *Ninamys* sp., cf. *N. annectens* from Obritsch Ranch. Measurements in mm. Abbreviations: L, anteroposterior length; W, transverse width; *, M1 or M2.

NDGS #	P3L	P3W	P4L	P4W	M1L	M1W	M2L	M2W	M3L	M3W
2407*					1.54	2.03				
2411*					1.6	1.92				
2963	0.91	0.96	1.79	2.03	1.39	2.08	1.42	2.10	—	—
4051	0.75	0.76	1.77	2.16	1.45	2.13				
Mean	0.83	0.86	1.78	2.10	1.50	2.04	1.42	2.10		

NDGS #	p4L	p4W	m1L	m1W	m2L	m2W	m3L	m3W
2403					1.56	—		
2406	1.50	—						
2408							1.56	1.41
2409	—	1.51						
2410			1.79	1.78				
2412			1.62	1.77				
2475							1.75	1.36
2498							1.90	1.45
2964					1.63	1.65		
Mean	1.50	1.51	1.71	1.78	1.60	1.65	1.74	1.41

and the hypolophid extends buccally from it. On the m1s, it curves posteriorly, meeting the posterior cingulid at its center forming a distinct hypoconulid. On the m2s, the hypolophid extends across the talonid basin, joining the ectolophid at the posterolingual corner of the mesoconid. The hypolophid is lower than the other lophs on the tooth. The hypoconid is obliquely compressed at the posterobuccal corner of the tooth. The ectolophid extends from the posterolingual corner of the protoconid to the anterior arm of the hypoconid, with a distinct, central mesoconid. On the heavily worn specimen of m2 (NDGS 2403), there is a short loph extending posteriorly from the center of the metalophid II into the center of the talonid. On the little worn specimens there is some irregularity of the enamel in the central basin, arising from the ectolophid.

The m3s are distinguished from the anterior molars by the posterior expansion of the tooth, posterior to the hypolophid, where the posterior cingulid bows posteriorly (Fig. 3F). The remainder of the occlusal morphology is very similar to that of m2. The posterior arm of the protoconid is long but ends just short of fusing with the base of the metaconid, forming a transversely elongated trigonid basin. The hypolophid is as in m2, joining the mesoconid, but is higher than in m2. On only one specimen (NDGS 2498) is

there an accessory mesostylid. On all the specimens, the larger mesostylid is separated from the posterior end of the metastylid crest and is relatively large.

Discussion.—This species is referable to *Ninamys* based on the diagnosis of the genus having a partial ectoloph on the upper molars, m1 and m2 wider than long, closed or nearly closed trigonid on the lower cheek teeth, and connection of the hypolophid to the mesoconid on m2 and m3 (Vianey-Liaud et al. 2013; Korth 2019). It is closest to the North American *N. annectens* in both size and morphology, is not as lophate as the Eurasian *N. kazimieri* and *N. daxnerae*, and has the mesostylid variably doubled as in *N. annectens*. Although there are no specimens of dentaries that preserve both m2 and m3 from the Obritsch Ranch sample, the average length of m3 is only about 5 percent greater than that of m2 (Table 2). In other species of *Ninamys*, as in *Prosciurus* and other prosciurines, the m3 is approximately 20 percent longer than m2. Because of the slight difference in size of the lower cheek teeth, the Obritsch Ranch sample of *Ninamys* is referred tentatively to *N. annectens*.

All other occurrences of *Ninamys* in North America are from the late Orellan (=early-middle Oligocene; Korth

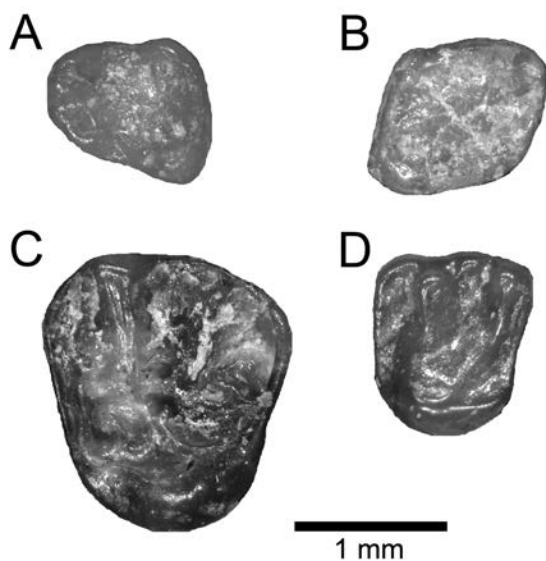


Fig. 4.—Cheek teeth of *Hesperopetes* and *Oligospermophilus* from Ob-ritsch Ranch. A–B, *H. blacki*. A, NDGS 2489, left p4; B, NDGS 2460, right m1 or m2. C, *H. jamesi*, NDGS 2481, left M3. D, *Oligospermophilus* sp., NDGS 2454, left M1 or M2.

1989, 2019), slightly older than the Eurasian occurrence where the genus ranges from the middle to late Oligocene (Vianey-Liaud et al. 2013).

Family Sciuridae Fischer de Waldheim, 1817

Subfamily uncertain

Genus *Hesperopetes* Emry and Korth, 2007

Hesperopetes blacki Emry and Korth, 2007
(Figs. 4A–B)

Referred Specimens.—NDGS 2489, left p4; NDGS 2460, right m1 or m2.

Occurrence.—Sampling interval 2.

Description.—The p4 is longer than wide (Fig. 4A), and the anterior width is greater than the posterior width (anteroposterior length = 1.16 mm; transverse width = 1.05 mm). The metaconid, protoconid, and anteroconid are closely packed along the anterior margin of the tooth and approximately equal in size; the anteroconid is situated between the other cusps, slightly smaller, and more anterior. A distinct mesostylid is near the center of the lingual side of the tooth, connected to the metaconid by a distinct lophid running along the lingual side of the tooth (=metastylid crest). The ectolophid is a low, anteroposteriorly running ridge along the buccal side of the tooth with a small, central, laterally compressed mesoconid. Numerous minute lophules fill the central basin of the tooth, radiating

from the lingual, posterior and buccal sides of the tooth. The posterior cingulid is a curved ridge that runs in an arc from the hypoconid to the entoconid around the posterior margin of the tooth. The hypoconid is small and slightly transversely compressed.

The only m1 is heavily worn (Fig. 4B), so little of the occlusal morphology is preserved, but there is evidence of the crenulated enamel in the talonid basin as well as a minute anteroconid and small, closed trigonid as in the topotypic material of this species (Emry and Korth 2007). In size (anteroposterior length = 1.25 mm; transverse width = 1.16 mm), it is similar in length to the holotype of the species, but is narrower transversely, apparently due to poor condition of the specimen (Emry and Korth 2007: table 1).

Discussion.—In size and morphology, these specimens do not differ from the type material from South Dakota, or the referred material from North Dakota (Emry and Korth 2007; Korth et al. 2019).

Hesperopetes jamesi Emry and Korth, 2007
(Fig. 4C)

Referred Specimen.—NDGS 2481, left M3.

Occurrence.—Sampling interval 2.

Measurements.—Anteroposterior length = 1.75 mm; transverse width = 1.85 mm.

Discussion.—The morphology of this tooth does not vary from that previously described for *H. jamesi* (Emry and Korth 2007). In size it is slightly smaller than the previously described specimens from the Whitneyan of South Dakota (Emry and Korth 2007: table 1; Korth 2014: table 7) but clearly larger than specimens of *H. blacki*. Korth et al. (2019) included a partial m3 from Fitterer Ranch in *H. blacki* that was slightly larger than typical for that species (USNM PAL 642820). It is possible the latter tooth belongs to *H. jamesi*.

Subfamily Cedromurinae Korth and Emry, 1991

Oligospermophilus Korth, 1987

Oligospermophilus sp.
(Fig. 4D)

Referred Specimen.—NDGS 2454, left M1 or M2.

Occurrence.—Sampling interval 2.

Measurements.—Anteroposterior length = 1.11 mm; transverse width = 1.37 mm.

Description.—The occlusal outline of the tooth is roughly rectangular, the width being slightly greater than the length (Fig. 4D). The anterior cingulum runs nearly the entire length of the tooth along the anterior margin to a point

even with the apex of the protocone. A small, anteroposteriorly compressed parastyle is present at the buccal end of the anterior cingulum. The protoloph runs from the anteroposteriorly compressed paracone to the anterobuccal corner of the protocone and is slightly curved posteriorly. There is no indication of a protoconule. The protocone is slightly crescentic and continuous from its posterobuccal corner with the metaloph that runs buccally and posteriorly to meet with the metacone along the buccal edge of the tooth. There is no distinct metaconule, but there is a minute wear facet near the center of the metaloph that would correspond with one. As with the paracone, the metacone is slightly anteroposteriorly compressed. At the center of the buccal margin of the tooth is a large mesostyle that is connected to the paracone by a low, curved lophule that runs from the posterobuccal corner of the paracone to the anterolingual corner of the mesostyle. The hypocone is a small swelling posterior and slightly buccal to the protocone. The posterior cingulum runs from the hypocone along the posterior margin of the tooth to the center of the posterior edge of the metacone.

Discussion.—The upper molar referred here differs little from those of other species of the genus (Korth 1987, 2014). However, it is markedly smaller than any previously reported upper molars (Korth 1987: table 1; Korth 2014: table 6). The only morphological difference between it and that of other species is that the metaloph is continuous with the protocone; it is either not continuous or only weakly so in other species. This specimen likely represents a new species of *Oligospermophilus* but cannot be named at this time due to its poor representation. Elsewhere, *Oligospermophilus* has been reported from the Chadronian and Orellan of Nebraska, and Whitneyan of Wyoming and South Dakota (Korth 1987, 2014).

Family Castoridae Hemprich, 1820
Genus *Oligotheriomys* Korth, 1998

Oligotheriomys magnus (Wood, 1937)
(Fig. 5)

Referred Specimen.—NDGS 2427, right M1 or M2.

Occurrence.—Sampling interval 2.

Measurements.—Anteroposterior length = 4.24 mm; transverse width = 5.85 mm; buccal crown-height = 2.08 mm; lingual crown-height = 4.89 mm.

Description.—The tooth is unilaterally hypsodont, the lingual height being more than double the buccal height (Fig. 5A). The tooth is moderately to heavily worn (both the mesoflexus and hypoflexus are still open). The occlusal surface has a long, central, J-shaped mesoflexus and a shallow hypoflexus that is angled anterobuccally (Fig. 5B). On the anterior half of the tooth are two smaller fossettes, a transversely elongated buccal fossette, and a circular lingual

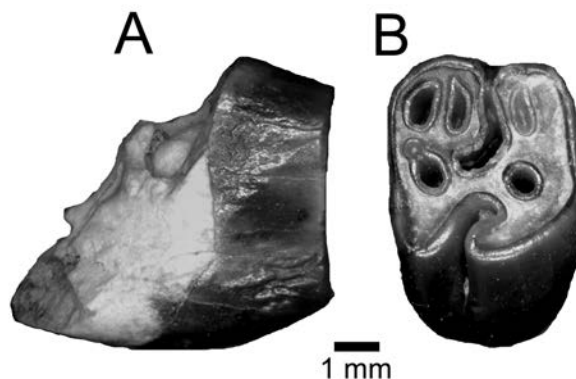


Fig. 5.—*Oligotheriomys magnus*, NDGS 2427, right M1 or M2. A, posterior view; B, occlusal view.

fossette. On the posterior half of the tooth three fossettes are present. On the buccal side are two small ovate fossettes (transversely elongated), and lingually there is a single large circular fossette that is continuous with a minute fossette that is connected to it along the posterobuccal edge.

Discussion.—This upper molar (NDGS 2427) is similar in size to that of the holotype of *O. primus*, FAM 64016 (Korth 1998; =*O. magnus*; see Korth et al. 2019). It differs from the latter in having a slightly less complex occlusal pattern with fewer fossettes. However, it appears that this difference is only due to the degree of wear on NDGS 2427. FAM 64016 has minimal wear (Korth 1998: fig. 1), whereas NDGS 2427 is more heavily worn, with some of the minor fossettes having been eliminated.

Family Eomyidae Winge, 1887
Genus *Adjidaumo* Hay, 1930

Adjidaumo minimus (Matthew, 1903)
(Figs. 6A–E; Table 3)

Referred Specimens.—NDGS 2367, 2370, 2377, 2453, 2492, P4; NDGS 2173, 2362, 2363, 2369, 2373, 2375, 2380, 2447, 2456, 2488, 4041, 4044, M1 or M2; NDGS 4046, M3; NDGS 2365, 2399, 2448, 2464, p4; NDGS 2167, 2364, 2368, 2372, 2374, 2379, 2451, 2486, 2487, 2494, 4042, 4043, 4047, m1 or m2; NDGS 2466, right m3.

Occurrence.—Sampling interval 2.

Discussion.—The dentition of *A. minimus* has been well described and documented from the Chadronian (Matthew 1903; Wood 1937; Black 1965; Korth et al. 2015), Orellan (Korth 2019), and Orellan/Whitneyan (Korth et al. 2019). The material from Obritsch Ranch most closely approaches that from the later occurring Fitterer Ranch, North Dakota (Korth et al. 2019). This is the third record of *A. minimus*

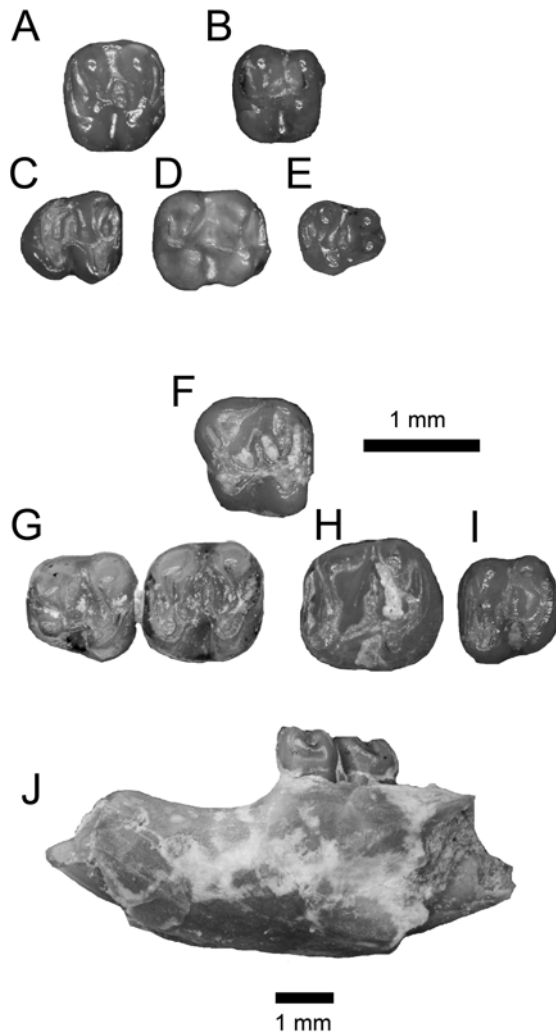


Fig. 6.—Cheek teeth and dentary of eomyids from Obritsch Ranch. **A–E**, *Adjidaumo minimus*. **A**, NDGS 2456, right M1 or M2; **B**, NDGS 2492, right P4; **C**, NDGS 2466, right m3; **D**, NDGS 2487, right m1 or m2; **E**, NDGS 2365, right p4. **F–J**, *Paradjidaumo obritschorum*. **F**, NDGS 2474, left P4; **G**, NDGS 2965 (holotype), left p4-m1; **H**, NDGS 2361, left m2; **I**, NDGS 2376, left m3; **J**, NDGS 2965 (holotype), lateral view of dentary. Anterior to right in A–E; anterior to left on F–J. Figure 6J to different scale (below).

from later than the Chadronian, the other references are from Montana (Tabrum et al. 1996; Korth 2019) and North Dakota (Korth et al. 2019), suggesting this species persisted in the northern montane areas of North America, and not in the central and northern plains.

Genus *Paradjidaumo* Burke, 1934

Paradjidaumo (Macroadjidaumo) obritschorum, new species
(Figs. 6F–J; Table 4)

Type Specimen.—NDGS 2965; left dentary with i1, p4-m1.

Referred Specimens.—NDGS 2474, left P4; NDGS 2457, m1; NDGS 2361, 2378, m2; NDGS 2366, 2376, m3.

Occurrence.—Sampling intervals 2 and 3

Diagnosis.—Small species, near size of *P. nanus*; p4 wider than long, proportionally shorter than in any other species ($L/W = 0.88$); high-crowned molars ($ht/W = 0.36$).

Etymology.—Named in recognition of the Obritsch family for their continued support of paleontological research by the North Dakota Geological Survey on their property.

Description.—The dentary is shallow (depth below m1 = 3.41 mm). The masseteric scar is typically a U-shape, ending anteriorly just below mid-depth of the dentary, below the center of p4 (Fig. 6J). The mental foramen is minute and just anterior of the center of the diastema, slightly below the dorsal surface of the diastema.

The incisor is much narrower across than deep (0.64 mm transverse width versus 1.27 mm depth). The enamel is along the nearly flattened anterior surface and extends up about one-third the lateral side.

The cheek teeth are high-crowned for the genus (mean $ht/width = 0.36$; range = 0.32–0.41), equaling that of the type species *P. trilophus* (Korth 2013: table 1), but are smaller than any other species. The p4 is only slightly shorter than long, and wider posteriorly than anteriorly (Fig. 6G). The protoconid and metaconid are equal in size and flattened medially. A minute, anteroposteriorly oriented trigonid basin is between the trigonid cusps and closed posteriorly and open narrowly, anteriorly. The hypoconid and entoconid are similarly equal in size, the hypoconid is crescentic in occlusal outline, and the entoconid oval (anteroposteriorly compressed). The ectolophid runs from the posterior side of the protoconid to the anterior hypoconid, forming a small V-shape. A short mesolophid extends from the apex of the V into the talonid basin. The posterior cingulid only consists of a very short lophid that extends directly posterior from the center of the hypolophid.

The m1 is nearly square in occlusal outline, being only slightly wider than long (Fig. 6G; Table 4). The width of the metalophid is slightly less than that of the hypolophid. The anterior cingulid is directly connected to the protoconid at its buccal end and extends lingually along the anterior margin of the tooth to a point just short of the apex of the metaconid. Both the metaconid and protoconid are anteroposteriorly compressed, and connected by a straight, transversely oriented metalophid that joins the apices of the cusps. The ectolophid is as in p4, forming a V-shape with a mesolophid at the apex extending lingually. The mesolophid is longer than that of p4 but does not reach the lingual side of the tooth. The hypoconid is crescentic, as in p4, but the entoconid is nearly circular in occlusal outline. The hypolophid bows posteriorly, running from the

TABLE 3. Dental measurements of *Adjidaumo minimus* from Obritsch Ranch. Measurements in mm. Abbreviations: CV, coefficient of variation; L, anteroposterior length; M, mean; Max, maximum measurement; Min, minimum measurement; N, number of specimens; SD, standard deviation; W, transverse width.

	P4L	p4W	M1 or M2L	M1 or M2W	M3L	M3W		
N	5	4	12	10	1	1		
M	0.80	0.86	0.91	0.98	0.62	0.84		
Min	0.74	0.75	0.83	0.90				
Max	0.88	0.90	1.01	1.03				
SD	0.06	0.07	0.05	0.05				
CV	7.28	8.24	5.30	4.92				

	dp4L	dp4W	p4L	p4W	m1 or m2L	m1 or m2W	m3L	m3W
N	1	0	4	3	12	12	1	1
M	0.67	—	0.80	0.71	0.97	0.93	0.87	0.81
Min	—	—	0.75	0.67	0.79	0.82	—	—
Max	—	—	0.90	0.74	1.06	1.06	—	—
SD	—	—	0.07	0.04	0.07	0.08	—	—
CV	—	—	8.54	5.31	6.88	9.08	—	—

TABLE 4. Dental measurements of *Paradjidaumo*. Measurements in mm. Abbreviations: L, anteroposterior length; W, transverse width.

<i>Paradjidaumo obritschorum</i>								
NDGS #	P4L	P4W						
2474	1.02	1.08						

NDGS #	p4L	p4W	m1L	m1W	m2L	m2W	m3L	m3W
2965	0.95	0.99	1.08	1.11				
2366							0.9	0.87
2376							0.89	0.95
2378					1.24	1.26		
2361					1.22	1.21		
2457			—	—				
Mean	0.95	0.99	1.08	1.11	1.23	1.24	0.90	0.91

<i>Paradjidaumo trilophus</i>									
NDGS #	p4L	p4W	m1L	m1W	m2L	m2W	m3L	m3W	p4-m3L
4050	1.56	1.31	1.31	1.35	1.26	1.36			5.77

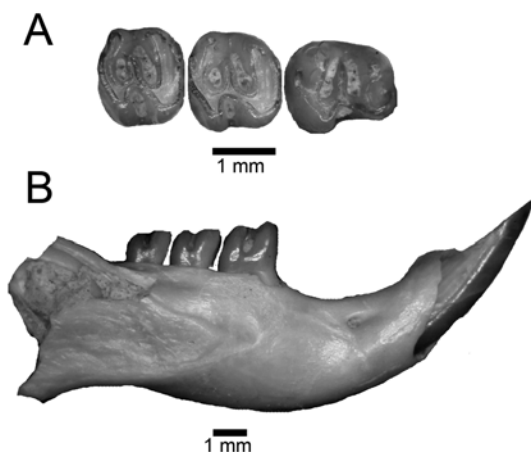


Fig. 7.—*Paradjidaumo trilophus* from Obritsch Ranch, NDGS 4050, right dentary with i1, p4–m2. **A**, occlusal view of p4–m2; **B**, lateral view of dentary. Anterior to right on both figures. Figures to different scales (below each figure).

posterolingual corner of the hypoconid to the posterobuccal corner of the entoconid. A short posterior cingulid originates from the hypolophid lingual to its center and ends at the level of the buccal edge of the entoconid.

The specimens referred to m2 differ from the m1 of the holotype in being slightly larger and having a shorter posterior cingulid (Fig. 6H), typical of other species of the genus. The mesolophid on the referred m2s is like that of m1 of the holotype and ends well short of the lingual side of the tooth.

The m3 is typically reduced in size with the posterior cingulid nearly absent and the hypoconid reduced in size relative to the anterior molars, making the tooth narrower posteriorly (Fig. 6I).

Discussion.—Other than its small size, *P. obritschorum* is referable to the subgenus *Macroadjidaumo* Korth, 2013, based on the relative size of p4 (only 88 percent the length of m1), m1 and m2 approximately equal in width and length (wider in subgenus *Paradjidaumo*), and the relatively higher crown-height of the molars. The specimens differ from the other known species of this subgenus in being slightly smaller (Table 4; Kelly 2010: table 4; Korth 2013: table 9), and having m1 and m2 essentially equal in width and length. In the other recognized species, *P. (M.) alberti* Russell, 1954, and *P. (M.) reynoldsi* Kelly, 1992, the m1 and m2 average from 2.5 to 7.0 percent longer than wide.

The Whitneyan occurrence of *P. (Macroadjidaumo)* at Obritsch Ranch is much later than the reported occurrences of the other species, being from the Duchesnean and Chadronian (Russell 1954; Kelly 1992; Korth 2013). Geographically, the occurrence of *P. (M.) obritschorum* is nearest that of *P. (M.) alberti* from southern Saskatchewan (Russell 1954).

Paradjidaumo (Paradjidaumo) trilophus (Cope, 1873a)
(Fig. 7; Table 4)

Referred Specimen.—NDGS 4050, right dentary with i1, p4–m2.

Occurrence.—Sampling interval 1.

Discussion.—The size and morphology of the lower cheek teeth does not differ from that of large samples of *P. trilophus* from other localities (Wood 1937; Black 1965; Korth 1980, 2013; Korth et al. 2019). The only variation is that the relative length of p4 to m1 ($p4L/m1L = 1.19$) is greater than previously reported for *P. trilophus* or any other species. The maximum for *P. trilophus* is 1.04, and for the genus is 1.12 (Korth 2013: table 5).

Family Heliscomyidae Korth et al., 1991
Genus *Heliscomys* Cope, 1873b

Heliscomys sp., cf. *H. vetus* Cope 1873b
(Figs. 8A–D; Table 5)

Referred Specimens.—NDGS 2393, 2493, M2; NDGS 2165, right m1; NDGS 2382, 4038, m2; NDGS 2390, right m3.

Occurrence.—Sampling interval 2.

Discussion.—This species is distinguished from other species of the genus by its small size (Table 5) and the lack of styler cusps on M2 (Wood 1935; Korth 1989, 1995). Although similar in size to specimens of *H. senex* from nearby Fitterer Ranch (Korth et al. 2019: table A10), M2 of the latter always has styler cusps, which are lacking on the specimens from Obritsch Ranch (Fig. 8A).

Heliscomys medius Korth, 2007
(Figs. 8E–K; Table 6)

Referred Specimens.—NDGS 2491, 4040, P4; NDGS 2162, 2163, 2381, 2473, 2485, 4034, 4037, M1; NDGS 2387, 2450, 4033, 4035, M2; NDGS 4039, left M3; NDGS 2164, 2166, 2384, 2388, 2391, 2465, 2468, 4045, m1; NDGS 2131, 2178, 2383, 2389, 2392, 2467, 2499, 4032, m2; NDGS 2386, right m3.

Occurrence.—Sampling interval 2.

Description.—Only one of the two specimens of P4 is complete, NDGS 4040 (Fig. 8H). NDGS 2491 has the paracone broken away. The tooth is dominated by a large, central hypocone. It is surrounded by a small, buccal metacone, anterocentral paracone, and lingual hypostyle. The latter three cusps are all much smaller than the hypocone (the hypostyle being the largest) and conical in shape.

M1 is the largest of the upper molars (Fig. 8G). The four main cusps (paracone, protocone, metacone, and hypocone)

TABLE 5. Dental measurements of *Heliscomys* sp., cf. *H. vetus* from Obritsch Ranch. Measurements in mm. Abbreviations: L, anteroposterior length; W, transverse width.

NDGS #	M2L	M2W
2493	0.66	0.83
2393	0.65	0.78

NDGS #	m1L	m1W	m2L	m2W	m3L	m3W
2165	0.85	0.80				
2382			0.69	0.77		
2390					0.62	0.60
4038			0.67	0.69		

are equal in size and circular in occlusal outline with a deep central transverse valley separating the cusps of the proto-loph from those of the metaloph. The paracone is slightly more buccally placed than the metacone. The anterior cingulum originates at the anterobuccal corner of the tooth, just anterior to the apex of the paracone and extends lingually to the anterolingual corner of the tooth where it bends posteriorly and follows the lingual margin of the tooth to the base of the hypostyle. At the anterolingual corner of the tooth is a minor swelling of the cingulum (=protostyle). There is a prominent hypostyle that is circular

in outline and only slightly smaller than the main cusps. Although aligned, the cusps of the proto-loph and metaloph are only weakly joined, with no distinct transverse loph. The posterior cingulum consists of a short loph originating from the posterobuccal margin of the hypocone and extending buccally to the posterobuccal corner of the tooth, never fusing with the metacone.

M2 is smaller than M1, nearly square in outline, but still wider than long. The four main cusps are arranged as in M1 (Fig. 8F). The anterior cingulum is continuous with the lingual cingulum wrapping around the anterobuccal

TABLE 6. Dental measurements of *Heliscomys medius* from Obritsch Ranch. Measurements in mm. Abbreviations: CV, coefficient of variation; L, anteroposterior length; M, mean; Max, maximum measurement; Min, minimum measurement; N, number of specimens; SD, standard deviation; W, transverse width.

	P4L	P4W	M1L	M1W	M2L	M2W	M3L	M3W
N	1	2	7	7	4	4	1	1
M	0.65	0.80	1.03	1.18	0.81	0.95	0.85	1.06
Min		0.78	0.95	1.07	0.76	0.91		
Max		0.81	1.16	1.28	0.85	0.98		
SD			0.07	0.08	0.05	0.04		
CV			7.04	7.06	5.79	3.72		

	m1L	m1W	m2L	m2W	m3L	m3W
N	8	7	8	8	1	1
M	1.07	1.00	0.94	1.02	0.70	0.76
Min	0.98	0.94	0.87	0.95		
Max	1.19	1.10	1.00	1.15		
SD	0.06	0.05	0.04	0.07		
CV	5.97	5.25	4.46	6.50		

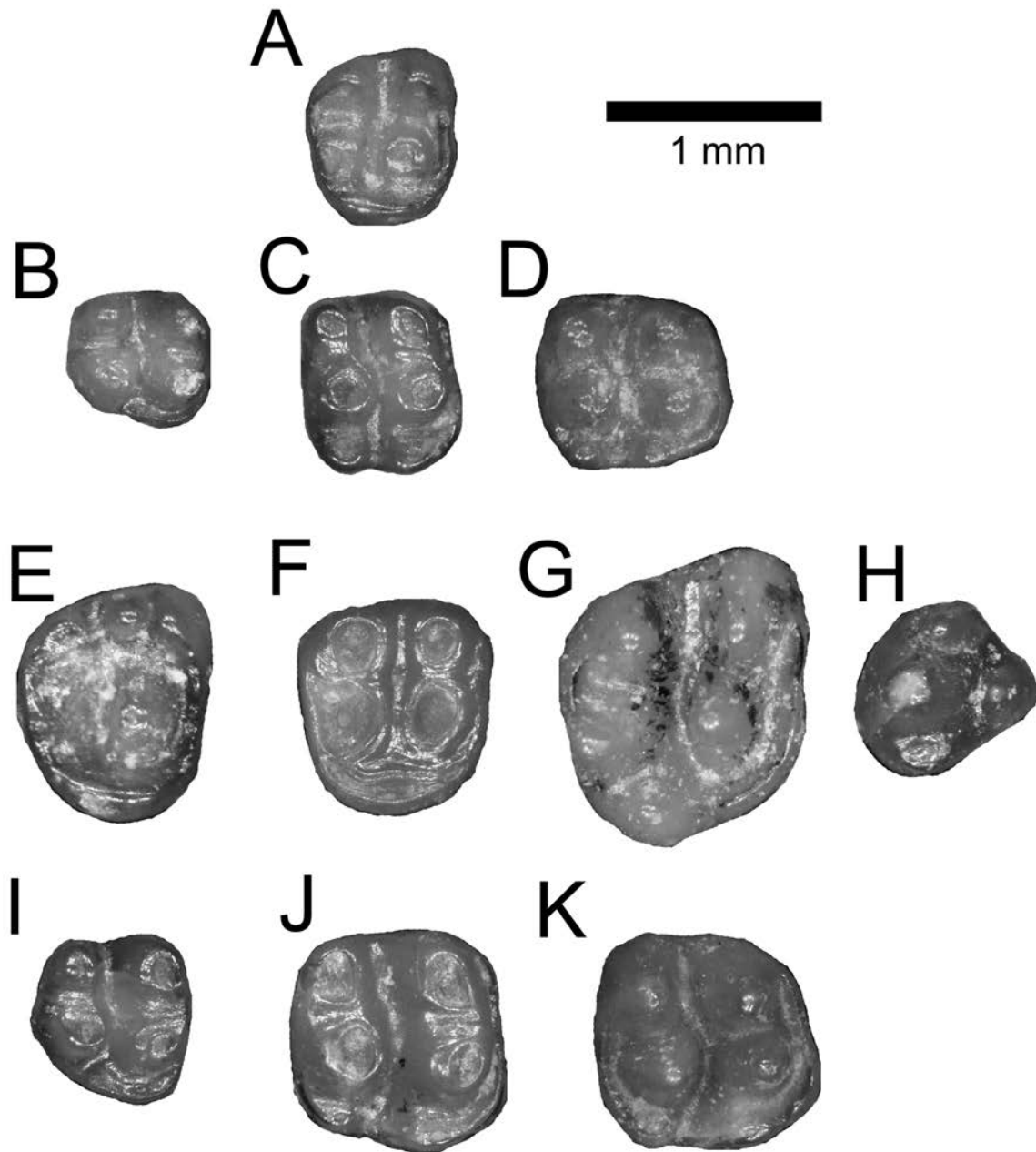


Fig. 8.—Cheek teeth of *Heliscomys* from Obritsch Ranch. **A–D**, *Heliscomys* sp., cf. *H. vetus*. **A**, NDGS 2393, left M2; **B**, NDGS 2390, right m3; **C**, NDGS 2382, right m2; **D**, NDGS 2165, right m1. **E–K**, *H. medius*. **E**, NDGS 4039 left M3 (reversed); **F**, NDGS 2387, right M2; **G**, NDGS 2162, right M1; **H**, NDGS 4040, left P4 (reversed); **I**, NDGS 2386, right m3; **J**, NDGS 2178, right m2; **K**, NDGS 2166, right m1. Anterior to right on all figures.

corner of the tooth and extending the full length of the tooth lingually, then turning buccally at the posterolingual corner of the tooth, joining the posterolingual corner of the hypocone. There are no distinct styler cusps, but there is a slight swelling on the cingulum, lingual to the hypocone.

The posterior cingulum is limited to a short, curved ridge that runs from the posterobuccal corner of the hypocone and joins the center of the posterior edge of the metacone.

Only one specimen, NDGS 4039, can be identified as an M3 of the species (Fig. 8E). The posterior half is reduced,

typical of other species. The paracone is slightly obliquely compressed, and continuous with the anterior cingulum that extends lingually from the anterolingual corner of the paracone. The cingulum wraps around the entire lingual side of the tooth, then extends along the posterior edge of the tooth, ending along the posterior side of the metacone. There is a large, isolated protocone near the center of the tooth that is only slightly anteroposteriorly compressed. At the center of the buccal border of the tooth is a large mesostyle. It is closely positioned posterior to the paracone and separated from the metacone by a narrow transverse valley. The most unusual feature of this cusp is its size; it is round in occlusal outline and equal to the paracone in size.

There are no specimens of p4 in the collection. The m1s and m2s can be separated from one another based on size (m1 larger) and proportions (m1 longer than wide; m2 wider than long). On m1, the major cusps are subequal in size (Fig. 8K), the hypoconid being only barely larger than the other cusps. The four main cusps (metaconid, protoconid, entoconid, and hypoconid) are arranged in two weakly developed transverse lophs, metalophid and hypolophid. The anterior cingulid originates along the anterior edge of the tooth anterior to the apex of the metaconid, extends lingually, then wraps around the anterobuccal corner of the tooth, extends posteriorly to a point approximately even with the protoconid where it ends in a small protostylid. There is a break in the buccal cingulid after the protostylid that is continuous with the central transverse valley of the tooth. Posterior to this break in the buccal cingulid, is a small hypostylid, variable in size but usually approximately equal to the protostylid. Extending from the posterior side of the hypostylid is a cingulid that bends around the posterobuccal corner of the tooth and continues along the posterior edge, ultimately fusing with the apex of the entoconid. The height of the posterior cingulid is variable and on a few specimens there is a minute cuspule along it between the hypoconid and entoconid (=hypoconulid).

In overall occlusal morphology, m2 is very similar to m1 (Fig. 8J). Other than the proportions of the tooth, the biggest difference appears to be in the development of the anterior and posterior cingulids. The anterior cingulid is lower than in m1 and more closely appressed to the metalophid. Similarly, the posterior cingulid is closer to the posterior side of the cusps of the hypolophid and is often interrupted by the posterior margin of the hypoconid, reappearing between the bases of the hypoconid and entoconid as a short lophulid.

There is only a single m3 available from this collection (NDGS 2386; Fig. 8I). It differs from the anterior molars in having a much reduced hypolophid. Both cusps are distinctly smaller than the metalophid cusps and the posterior width is narrower than the anterior width. The anterior cingulid is reduced to a short loph between the metaconid and protoconid, and the buccal cingulid is a low ridge around the anterobuccal corner that ends posteriorly before reaching the posterobuccal corner of the tooth. There are no distinct cingulid cusps.

Discussion.—This is the first recognition of lower molars of *H. medius*, which has previously been known only from upper cheek teeth (Korth 2007; Korth et al. 2019). The lower molars do not differ markedly from those of other species of *Heliscomys* but are assigned here to *H. medius* based on size and likely association with the recognized upper teeth from Obritsch Ranch.

The specimens from Obritsch Ranch differ from the type material from South Dakota only in the slightly better development of the hypostyle on P4 (Korth 2007: fig. 3A). The average width of P4 relative to that of M1 for the Obritsch Ranch sample is 67%, only slightly larger than that previously reported for *H. medius* (50–64%; Korth 2007). In size, this species is larger than specimens of *H. borealis* from nearby Fitterer Ranch (Table 6; Korth et al. 2019: table A12).

Family Heteromyidae Gray, 1868
Subfamily Harrymyinae Wahlert, 1991
Genus *Proharrymys* Korth and Branciforte, 2007

Proharrymys sp., cf. *P. fedti* (Macdonald, 1963)
(Figs. 9–11; Tables 7–8)

Referred Specimen.—NDGS 2962, partial cranium with rostrum, palate, both orbital walls and parietals, incisors and left and right P4–M3.

Occurrence.—Sampling interval 3.

Description of cranium.—Dorsal: The nasals are lacking but their outline is preserved along the nasal-premaxillary suture (Fig. 9A). The nasals are narrow and parallel-sided, flaring only slightly at the anterior end. They extend posteriorly approximately to the anterior edge of the orbit. The nasofrontal suture forms a zig-zag pattern. The premaxillaries extend just slightly more posteriorly with a similar suture pattern with the frontal. The maxilla is lateral to the premaxilla but does not extend as far posteriorly. The dorsal surfaces of the frontals are flat, but there is no indication of a supraorbital flange. The minimum postorbital width is near the center of the anteroposterior length of the frontals, which flare posteriorly. Only a fragment of the frontal-parietal suture is preserved on the right side of the skull.

Lateral: The diastema is 8.00 mm in length with a flat ventral surface that curves slightly downward just posterior to the incisors (Fig. 9C). The zygomatic arch is fully sciuriformous, sloping anterodorsally. The maxillary-premaxillary suture runs from the anterodorsal point of the maxilla, sloping slightly anteriorly for about half the depth of the rostrum, then slopes slightly posteriorly to the base of the rostrum. The infraorbital foramen is expanded anteriorly by a rostral perforation (height = 1.6 mm; length = 1.4 mm). It is oriented nearly vertically, with a slight anterodorsal tilt. Posterior and ventral to the infraorbital foramen is a slight swelling for the attachment of the masseter.

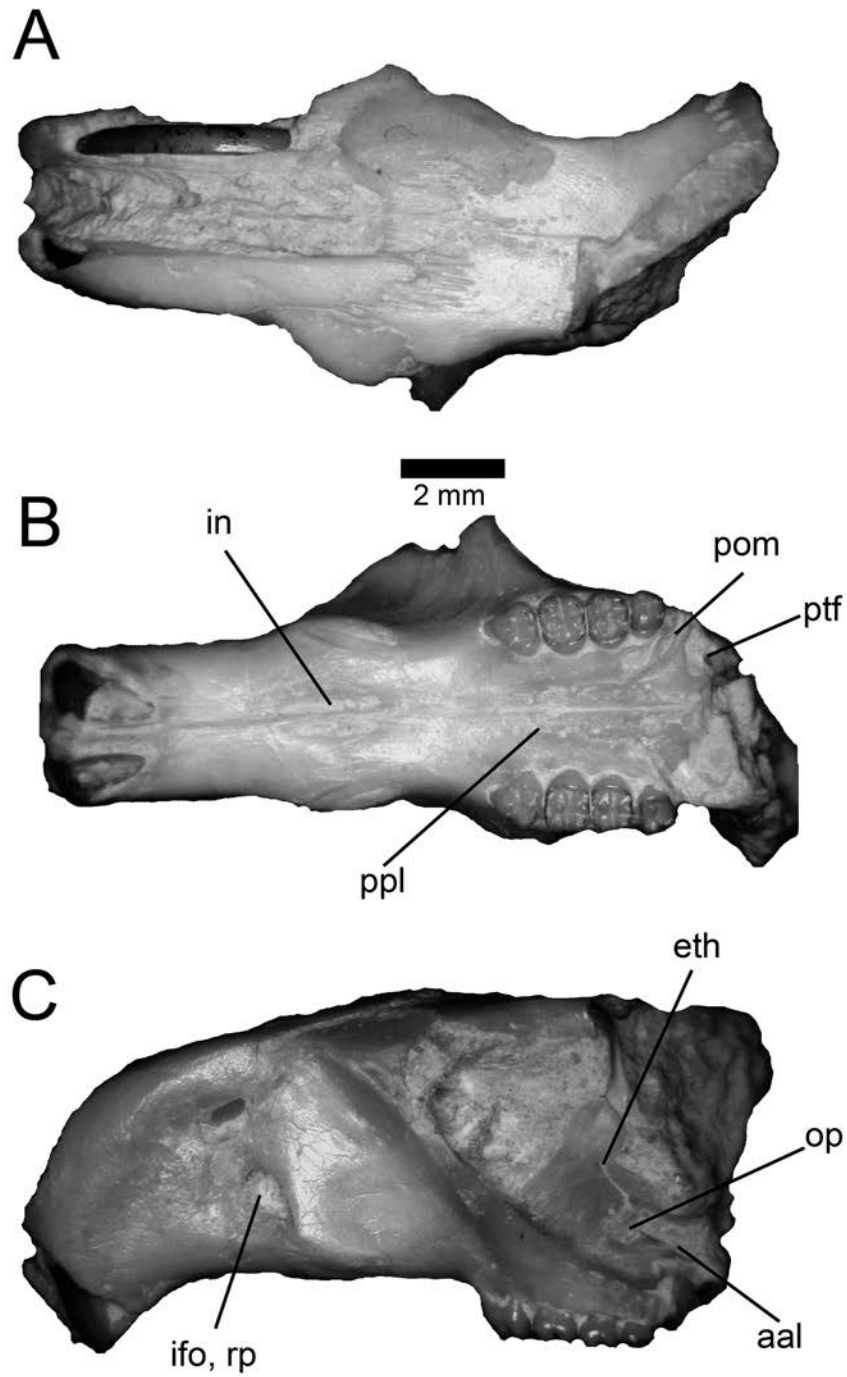


Fig. 9.—*Proharrymys* sp., cf. *P. fedti*, NDGS 2962, partial cranium from Obritsch Ranch. **A**, dorsal view; **B**, ventral view; **C**, left lateral view. Anterior to the left on all figures. Abbreviations: aal, anterior alar fissure; eth, ethmoid foramen; ifo, infraorbital foramen; in, incisive foramen; op, optic foramen; pom, posterior maxillary foramen; ppl, posterior palatine foramen; ptf, pterygoid fossa; rp, rostral perforation.

Much of the orbital wall is missing particularly in the anterodorsal corner in the area of the lacrimal foramen. The frontal-maxillary suture runs posteroventrally from the anterodorsal corner of the orbit as an irregular line. A small opening for the infraorbital canal (ifc) is dorsal to the anterior margin of M1 just below the frontal-maxillary suture (Fig. 10B). It is blocked laterally by the base of the zygomatic arch and is only visible from above. Posterior and ventral to the posterior opening for the infraorbital canal is the sphenopalatine foramen (spl) within the maxilla, just above M1. Dorsal to M2, and much higher, is a small ethmoid foramen which is within the frontal-orbitosphenoid suture (Figs. 9C, 10A). The dorsal palatine foramen (dpl) is along the maxillary-palatine suture, dorsal to M2. The alisphenoid is along the posterior wall of the orbit and extends well dorsal to the ethmoid foramen (eth). Ventral and slightly posterior to the ethmoid foramen is an oval optic foramen (op) within the orbitosphenoid, dorsal to M3. The anterior opening of the sphenoidal fissure is just posterior and ventral to the optic foramen, dorsal to M3 (only preserved on the right side of the skull).

Ventral: The incisive foramina (in) are near the center of the anteroposterior length of the diastema (Fig. 9B) and are approximately 31% the total length of the diastema. They are narrow, elongated slits situated along the centerline. The swelling for the attachment of the masseter is directly lateral to the foramen. The maxillary-premaxillary suture is irregular (zig-zag) and intersects the incisive foramen just anterior to its posterior margin. It extends laterally, reaching the anterior margin of the attachment of the masseter, and its path never extends posterior to the incisive foramen. The palatal surface between the tooth rows is slightly concave upward, but nearly flat. The palatine extends anteriorly to the level of the posterior part of P4. There are multiple posterior palatine foramina (ppl). The most anterior are within the maxilla, along the palatine-maxillary suture. Posterior to these, on both sides of the palate, are several additional, smaller foramina. The first is very small and just posterior to the anterior foramen, along the suture, but within the palatine. Posterior to it is another larger foramen, entirely within the palatine, medial to the

TABLE 7. Cranial measurements of *Proharrymys* sp., cf. *P. fedti*, NDGS 2962. Measurements in mm.

Length of diastema	8.00
Length of incisive foramen	2.51
Anterior rostral width	4.52
Posterior rostral width	5.23
Maximum rostral height	7.08
Width of postorbital constriction	5.20
Height of cranium at M2	7.59

TABLE 8. Dental measurements of *Proharrymys* sp., cf. *P. fedti*, NDGS 2962. Measurements in mm. Abbreviations: L, anteroposterior length; W, transverse width.

	Left	Right
P4L	1.13	1.13
P4W	1.24	1.25
M1L	1.02	1.00
M1W	1.35	1.41
M2L	0.98	0.97
M2W	1.29	1.31
M3L	0.84	0.85
M3W	1.10	1.11
P4-M3L	4.13	4.29
I1L	2.07	2.03
I1W	2.06	2.08

suture. The most posterior foramina are minute, entirely within the palatine, and aligned directly posterior to the larger foramina. On the left side, there appear to be two minute foramina and three on the right. On the left side, the posterior maxillary foramen (pom) is an elongated slit that extends lingually from the lateral side of the palate just posterior to M3, for slightly more than the width of the tooth. On the right side the foramen is closed laterally, but on the left side this cannot be determined due to damage of the specimen. Posterior to the posterior maxillary foramen is a larger depression (=pterygoid fossa).

Description of dentition.—The cheek teeth are brachydont and follow the general pattern of geomyoid rodents with two transverse rows of cusps, separated by a deep central valley (Fig. 11). P4 is submolariform. The proto-loph consists of a large, central protocone and a smaller paracone on its anterolingual slope. The proto-loph is separated from the metaloph by a deep transverse valley that curves anteriorly at its lingual end, separating the protocone from the hypostyle. The metacone, hypocone, and hypostyle form a continuous loph. The metacone is anteroposteriorly compressed along the buccal margin of the tooth. The hypocone is the largest of the cusps, circular in outline, and centered along the posterior margin of the tooth. The hypostyle is anteriorly elongated and continuous posteriorly with the hypocone. A short posterior cingulum is low on the crown, along the posterior margin of the tooth between the apices of the metacone and hypocone.

M1 is the largest of the molars and its occlusal surface is dominated by the proto-loph and metaloph, both consisting of two large, transversely aligned cusps. The central transverse valley is blocked lingually by the lingual cingulum.

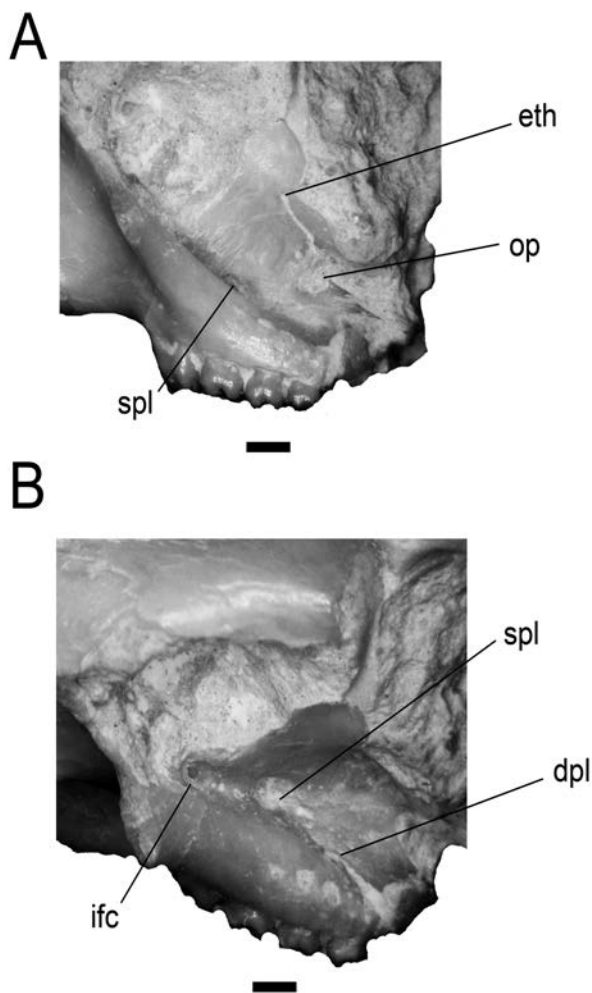


Fig. 10.—Medial orbital wall of cranium of *Proharrymys* sp., cf. *P. fedti*, NDGS 2962. **A**, lateral view; **B**, dorsolateral view. Abbreviations: dpl, dorsopalatine foramen; eth, ethmoid foramen; ifc, infraorbital canal; op, optic foramen; spl, sphenopalatine foramen. Scale bars = 2 mm.

The anterior cingulum is low on the tooth, originating buccally anterior to the paracone and extending lingually along the anterior side of the tooth before wrapping around the lingual side, ending at the posterolingual corner of the hypocone. However, there is a shallow break in the cingulum lingual to the protocone. Just anterior to this break is a small, compressed styler cusp. Posterior to the break is the larger entostyle that is a laterally compressed swelling along the lingual cingulum. A short posterior cingulum runs along the posterior margin of the tooth from the posterolingual corner of the hypocone for a short distance, ending at a point even with the apex of the metacone.

M2 is slightly smaller than M1, and shorter anteroposteriorly. It has the same general occlusal pattern as that of M1 but lacks the styler cusps and posterior cingulum of the latter.

M3 is the smallest of the molars. The cusps of the proto-loph and lingual cingulum are as in M2. The posterior half of the tooth is greatly reduced. The metacone is a slight swelling along the buccal margin of the tooth, posterior to the paracone. The hypocone is barely recognizable as a low, round swelling in the center of the basin formed by the proto-loph and posterior margin of the tooth.

Discussion.—The upper cheek teeth of NDGS 2962 most closely approach those of the early Arikareean *Proharrymys wahlerti* Korth and Branciforte, 2007, in morphology. However, they differ in the presence of styler cusps and in being slightly larger in size (Table 8; Korth and Branciforte 2007: table 7). Two other species have been referred to this genus, “*Proheteromys*” *fedti* Macdonald, 1963, from the early Arikareean of South Dakota and “*Heliscomys*” *schlaikjeri* Black, 1961, from the Arikareean of Wyoming. The former is known only from a single dentary (Macdonald 1963), and the latter from a single maxilla with P4–M2 (Black 1961). The NDGS specimen differs from *P. wahlerti* in being larger and differs from both *P. wahlerti* and “*H.*” *schlaikjeri* in having distinct styler cusps on M1. NDGS 2962 is closest in size to “*Proheteromys*” *fedti*, but because it is known only from lower dentition, no direct comparisons can be made. Therefore, NDGS 2962 is referred only tentatively to *P. fedti* until additional specimens can be recovered for comparison.

Generic allocation of *Heliscomys schlaikjeri*.—Black (1961) named *Heliscomys schlaikjeri* from the Arikareean of Wyoming based on a maxillary fragment with P4–M2 (MCZ 7335), including it in the family Heteromyidae. He noted that it was larger than other species of the genus and it was the latest known occurrence for the genus at the time. More than two decades later, Wahlert (1984) named a new, primitive genus of florentiamyid, *Kirkomys*, and referred “*H.*” *schlaikjeri* to it. After another two decades, Korth and Branciforte (2007) named a new genus of heteromyid, *Proharrymys*, and transferred “*H.*” *schlaikjeri* to it along with “*Proheteromys*” *fedti* from the Arikareean of South Dakota. Since that time, “*H.*” *schlaikjeri* has been included in either *Kirkomys* or *Proharrymys* without discussion (Flynn et al. 2008; Korth 2008, 2014). No additional material of “*H.*” *schlaikjeri* has ever been recovered,

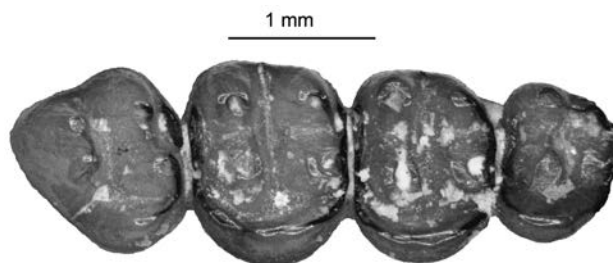


Fig. 11.—Upper left cheek teeth of *Proharrymys* sp., cf. *P. fedti*, NDGS 2962. Anterior is to the right.

TABLE 9. Dental measurements of *Eumys brachyodus* from Obritsch Ranch. Measurements in mm. Abbreviations: CV, coefficient of variation; L, anteroposterior length; M, mean; Max, maximum measurement; Min, minimum measurement; N, number of specimens; SD, standard deviation; W, transverse width.

	M1L	M1W	M2L	M2W	M3L	M3W	M1-M3L	
N	4	6	8	8	6	6	3	
M	3.12	2.13	2.21	2.15	1.80	2.01	7.27	
Min	2.93	1.92	2.05	1.92	1.68	1.80	7.06	
Max	3.43	2.24	2.51	2.25	1.91	2.29	7.54	
SD	0.22	0.12	0.16	0.13	0.08	0.17	0.24	
CV	7.00	5.61	7.16	5.90	4.50	8.20	3.36	

	m1L	m1W	m2L	m2W	m3L	m3W	m1-m3L	m1 W/L
N	22	23	34	34	33	30	26	22
M	2.45	1.90	2.23	2.11	2.40	2.05	7.05	0.77
Min	2.22	1.72	1.91	1.91	2.18	1.84	6.30	0.72
Max	2.67	2.15	2.47	2.35	2.66	2.25	7.53	0.83
SD	0.14	0.12	0.13	0.11	0.13	0.11	0.27	0.03
CV	5.64	6.34	5.90	5.36	5.45	5.22	3.86	4.08

so all generic (and familial) allocations have been based on the holotype.

In dental morphology, the upper cheek teeth of the holotype of “*H.*” *schlaikjeri* have a basic geomyoid pattern of transverse rows of cusps separated by a central transverse valley, and are like that of *Heliscomys*, *Kirkomys*, and *Proharrymys*. One of the features that Wahlert (1984) noted that separated *K. schlaikjeri* from the type species was the curvature of the base of the zygomatic arch. In the type species, *K. milleri* (later referred to *K. nebraskensis* [Wood, 1937], by Korth and Branciforte [2007]), the maximum curvature of the posterior margin of the zygomatic arch was anterior to the tooth row, and in *K. schlaikjeri* it was lateral to P4 (Wahlert 1984: figs. 2–3). The same position of curvature (anterior to the tooth row) as in *K. nebraskensis* (= *milleri*) has been figured for species of *Kirkomys* elsewhere (Korth and Branciforte 2007: fig. 5B; Korth 2014: fig. 8C). The position of the zygomatic arch in the skull of *Proharrymys* described herein is even with the anterior margin of P4, more like that of the type of “*H.*” *schlaikjeri* and *Proharrymys*. Due to this similarity in morphology, it appears best to refer “*H.*” *schlaikjeri* to *Proharrymys*.

Family Cricetidae Fischer de Waldheim, 1817
 Subfamily Eumyinae Simpson, 1945
 Genus *Eumys* Leidy, 1856

Eumys brachyodus Wood, 1937
 (Fig. 12; Table 9)

Referred Specimens.—NDGS 4010, skull fragment (palate) with right I1, M1–M3 and left I1, M1–M2; NDGS 2989, 4005, 4009, 4052, maxilla with M1–M3; NDGS 4003 maxilla with M2–M3; NDGS 4004, partial maxilla with I1, partial M1; NDGS 3000, maxillary fragment with partial M1; NDGS 4054, M1; NDGS 2978, 2980, 2981, 2985, 2987, 2988, 2994, 4001, 4002, 4011, 4015, dentary with i1, m1–m3; NDGS 2983, 2990, 2992, 2995, 2997–2999, 4006, 4008, 4012, 4016, 4053, dentary with m1–m3; NDGS 2979, 2986, 2991, 2993, 2996, 4007, 4013, 4014, partial dentary with m2–m3; NDGS, 4018, 4048, dentary with i1, m1–m2; NDGS 4017, partial dentary with i1, m1; NDGS 2982, dentary fragment with m2.

Occurrence.—Sampling intervals 1–3.

Discussion.—The sample of *Eumys brachyodus* from Obritsch Ranch differs very little in size or morphology from other large samples of *E. brachyodus* previously reported from South Dakota (Korth 2010a), Nebraska (Korth 2018), and North Dakota (Korth et al. 2019). As with other populations of *E. brachyodus*, it is similar in size to the Orellan *E. elegans* but differs from it in the proportions of m1 (wider relative to length than *E. elegans*; Korth 2010a: table 2, appendix; Korth 2018: tables 1–2; Korth et al. 2019: tables A13, A14) and morphology of the anteroconid

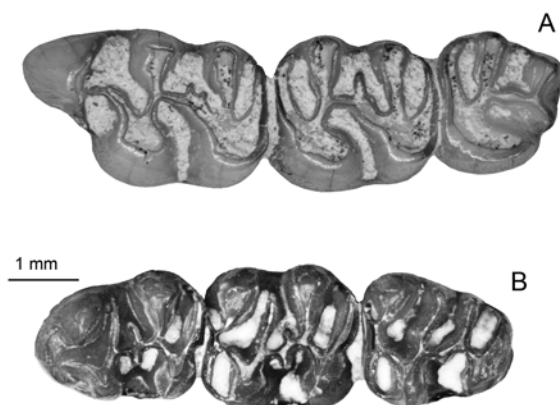


Fig. 12.—Cheek teeth of *Eumys brachyodus* from Obritsch Ranch. **A**, NDGS 2989, left M1–M3; **B**, NDGS 2990, left m1–m3. Anterior is to the right.

and metalophid on m1 (more commonly doubled in *E. brachyodus*: Korth 2018: fig. 6; Korth et al. 2019: fig. 15). In size, the dental measurements of the Obritsch Ranch sample most closely compares with that of the North Dakota sample (Korth et al. 2019: tables A13, A14), averaging slightly larger in all measurements than the Nebraska and South Dakota samples, but not significantly so. The double connection of the metalophid to the anteroconid on m1 of the Obritsch Ranch sample occurs in 16 percent of the specimens, slightly less than in the other samples of *E. brachyodus*, which occur from 19 to 38 percent of the specimens; clearly much more than in *E. elegans* (Korth 2018: fig. 6).

Genus *Scottimus* Wood, 1937

Scottimus sp., cf. *S. ambiguus* (Korth, 1981)
(Figure 13; Table 10)

Referred Specimens.—NDGS 2398, right M2; NDGS 2404, left M3; NDGS 2446, left m1; NDGS 2405, 4036 (partial) m2; NDGS 2400, 2402, m3.

Occurrence.—Sampling interval 2.

Description.—M2 (NDGS 2398) is longer than wide and heavily worn (Fig. 13A). The anterior cingulum extends for nearly the entire width of the tooth along the anterior border ending just short of the buccal and lingual edges. The buccal cusps (paracone, metacone) are slightly anteroposteriorly compressed, while the lingual cusps are larger and circular in occlusal outline. The anterior arms of the paracone and protocone join the anterior cingulum just lingual to its center. A longitudinal loph extends directly posteriorly from the center of the paracone to the center of

the metacone. Similarly, the endoloph extends posteriorly from the posterior arm of the protocone to the anterior arm of the hypocone, paralleling the buccal loph. The metaloph runs directly transversely from the center of the metacone to the center of the hypocone. The posterior cingulum runs from the posterobuccal corner of the hypocone to the buccal edge of the tooth, but does not fuse with the metacone.

The only m1 (NDGS 2446) is little-worn. It is elongated and narrower anteriorly than posteriorly (Fig. 13B). The anteroconid is central at the anterior end of the tooth and connected via a narrow lophid to the anterobuccal side of the metaconid. The metaconid is obliquely compressed and there is a distinct lophid running directly posterior from it along the lingual margin of the tooth which ends before reaching the entoconid. The protoconid is oval in outline and connected to the center of the posterior edge of the metaconid by an extension of the posterior arm of the protoconid that curves slightly anteriorly. The ectolophid runs posteriorly and slightly buccally to join the anterior arm of the hypoconid. There is no distinct mesoconid, but a short mesolophid extends lingually from the center of the ectolophid, ending well short of the base of the metaconid. The entoconid is oval in outline and obliquely oriented, its anterobuccal arm joining the ectolophid just posterior to its center. The hypoconid is crescentic in outline. The posterior arm of the hypoconid extends lingually for a short distance but does not reach the entoconid. Just short of the end of the posterior arm of the hypoconid is a lophid that extends directly posteriorly and joins the posterior cingulid, which runs to the edge of the tooth and joins the apex of the entoconid lingually from this junction, but only a short distance buccally.

The only complete m2 (NDGS 2405) is so heavily worn that no details of the occlusal surface can be determined. This tooth was referred to this species only based on its similar size although its dimensions have likely been greatly reduced by the extreme wear.

There are two specimens referable to m3, NDGS 2400 and NDGS 2402, the former being complete, the latter

TABLE 10. Dental measurements of *Scottimus* sp., cf. *S. ambiguus* from Obritsch Ranch. Measurements in mm. Abbreviations: L, anteroposterior length; W, transverse width.

NDGS #	M2L	M2W				
2398	1.57	1.42				
NDGS #	m1L	m1W	m2L	m2W	m3L	m3W
2405			1.01	0.78		
2400					1.80	—
2402					1.53	1.14
2446	1.85	1.19				

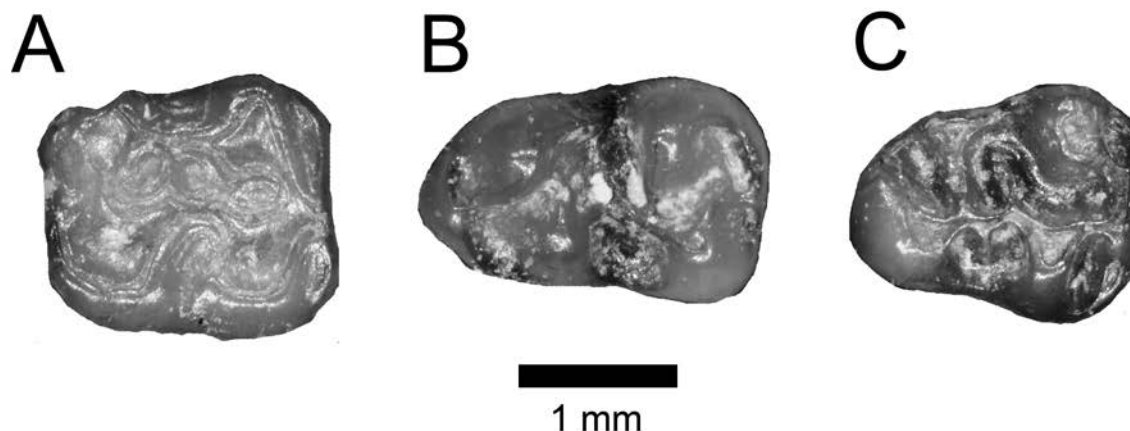


Fig. 13.—Molars of *Scottimus* sp., cf. *S. ambiguus* from Obritsch Ranch. **A**, NDGS 2398, right M2; **B**, NDGS 2446, left m1; **C**, NDGS 2402, left m3. Anterior to right in A and C, to the left in B.

being heavily worn and partially broken. The anterior half of NDGS 2400 resembles that of m2 (Fig. 13C). The anterior arms of the protoconid and metaconid join the anterior cingulid, but unlike m2, they do not meet one another but attach to the cingulid separately. The posterior arm of the protoconid (=metalophulid II) extends lingually, not quite reaching the lingual edge of the tooth. A low lophid extends posteriorly from the lingual side of the metaconid along the lingual edge of the tooth, joining the entoconid. The posterior half of the tooth is much narrower than the metalophid. Both the entoconid and hypoconid are reduced in size, particularly the former. The ectolophid extends directly posteriorly from the posterior arm of the protoconid to the anterior arm of the hypoconid. A distinct ectomesolophid extends buccally from its center. The hypolophid runs anterobuccally from the entoconid, joining the ectolophid at the anterolingual corner of the hypoconid. The posterior cingulid originates at the posterolingual arm of the hypoconid and wraps around the posterior end of the tooth, joining the posterior side of the entoconid along the lingual margin.

Discussion.—The morphology of the molars referable to *Scottimus* from Obritsch Ranch does not differ from that of other species of the genus. However, there is some difference in the size of the molars relative to previously described species. In overall size, the Obritsch Ranch material is smaller than previously described species, most nearly approaching the dental dimensions of *S. ambiguus* (Table 10; Korth, 1981: tables 3, 4). However, both the M3 and m3 from the Obritsch Ranch sample are proportionally smaller, relative to the anterior molars than in other species. It is likely that the Obritsch Ranch material represents a new species, but it is too poorly known at this time (seven isolated molars). For convenience, the material is tentatively referred to the otherwise Orellan *S. ambiguus*.

CONCLUSIONS

Variation between sampling intervals at Obritsch Ranch.—There are some minor changes in the rodents recovered from different sampling intervals at Obritsch Ranch; however, there is some inherent sampling error involved owing to the collection methods employed at each sampling interval, as was outlined above. Those differences could impact the resulting faunal data in several ways. First, sampling intervals 1 and 3 are likely to be biased towards collection of larger-bodied rodent taxa (e.g., *Eumys*, *Ischyromys*), while sampling interval 2 is likely to be biased towards smaller-bodied rodent taxa (e.g., *Adjidaumo*, *Heliscomys*). Second, the higher rodent diversity noted from sampling interval 2 (Fig. 14) is likely influenced in part by the more intensive sampling methods employed. Those factors make it difficult to say with certainty what the full stratigraphic ranges of small-bodied taxa (e.g., *Heliscomys medius*) are at Obritsch Ranch. Alternatively, the absence of rodent taxa from sampling interval 2 that are present in one of the other sampling intervals is more likely to be significant given the more intensive sampling methods employed on those rocks.

Ischyromys typus and *Eumys brachyodus* are the only species present in all sampling intervals at Obritsch Ranch (Fig. 14). *Paradjidaumo trilophus* is restricted to sampling interval 1 and is replaced in the local section in sampling intervals 2 and 3 by the smaller species *Paradjidaumo obritschorum*. Other species with restricted stratigraphic distributions include *Ninamys* sp., cf. *N. annectens* (sampling intervals 1 and 2) and *Proharrymys* sp., cf. *P. fedti* (sampling interval 3). In the cases of both *P. trilophus* and *P. cf. P. fedti*, if these species were present in sampling interval 2 it is likely that some evidence would have been recovered. Overall, only minor changes in the rodent assemblage at Obritsch Ranch through time are noted in this study.

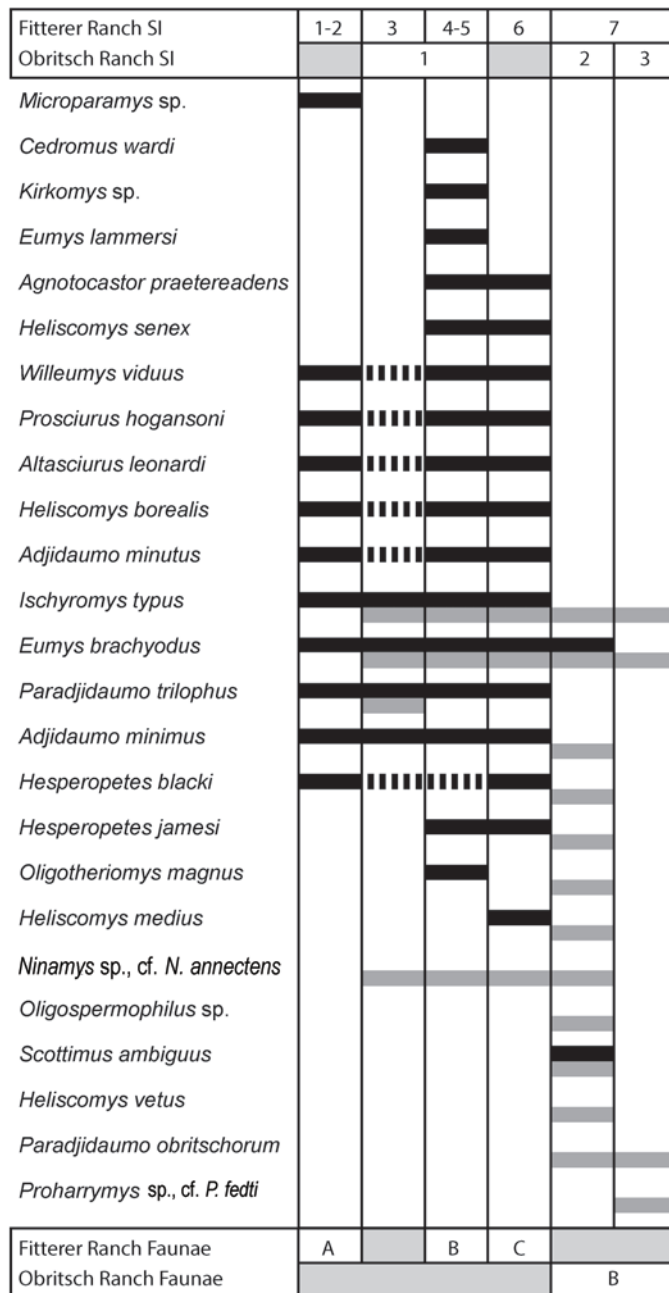


Fig. 14.—Stratigraphic distribution of rodent taxa within the Brule Formation at the Fitterer Ranch and Obritsch Ranch paleontological localities in Stark County, North Dakota. Black lines indicate occurrence at Fitterer Ranch, gray lines indicate occurrence at Obritsch Ranch, and dashed lines indicate inferred presence of a taxon based on presence in older and younger sampling intervals. Abbreviations: SI, sampling intervals.

Comparison of Obritsch Ranch and Fitterer Ranch rodent assemblages.—The rodent assemblage at Fitterer Ranch was recently described from stratigraphically controlled samples collected from seven distinct sampling intervals (Korth et al. 2019). The vertical extent of well-exposed outcrops of the Brule Formation varies between these two locations (Murphy et al. 1993), with the exposed

Fitterer Ranch section extending slightly lower (older) and the exposed Obritsch Ranch section extending slightly higher (younger). The overall rodent assemblage at Fitterer Ranch is similar in age to the Obritsch Ranch rodent assemblage, with both localities preserving largely Whitneyan faunae (Korth et al. 2019; this study). In terms of the composition of the rodent assemblages from these two

TABLE 11. Whitneyan rodent species and their distributions in well-described North American faunas. Abbreviations: †, species also reported from other locations; Ar, Arikareean biozone; BA, Blue Ash local fauna; CP, Cedar Pass local fauna; FRA, Fitterer Ranch Fauna A; FRB, Fitterer Ranch Fauna B; FRC, Fitterer Ranch Fauna C; HR, Harris Ranch units B through D; IP, inferred presence of species based on presence in older and younger faunas; NBU, species is not biostratigraphically useful as it is present in older and younger faunas; Or, Orellan biozone; ORB, Obritsch Ranch Fauna B; SB, Slim Buttes unit F; WH, White Hills local fauna.

Taxon	Or	WH	FRA	FRB	FRC	ORB	SB	CP	HR	BA	Ar	
<i>Agnotocastor coloradensis</i>	X										X	IP
<i>Metadjidaumo hendryi</i>	X										X	
<i>Eumys elegans</i>	X								X		X	NBU
<i>Adjidaumo minimus</i>	X		X	X	X	X						Whitneyan Last Appearances (LADs)
<i>Adjidaumo minutus</i>	X		X	X	X							
<i>Altasciurus relictus</i> †	X	X										
<i>Cedromus wardi</i>	X			X								
<i>Cedromus wilsoni</i>	X									X		
<i>Dakotallomys lillegraveni</i>	X						X					
<i>Eumys parvidens</i>	X									X		
<i>Heliscomys gregoryi</i>	X	X										
<i>Heliscomys senex</i>	X				X							
<i>Heliscomys vetus</i>	X					X						
<i>Ischyromys typus</i> †	X		X	X	X	X		X	X			
<i>Leptoromys wilsoni</i>	X						X					
<i>Ninamys annectens</i>	X					X						
<i>Oligotheriomys magnus</i>	X			X		X						
<i>Paradjidaumo trilophus</i>	X		X	X	X			X	X	X		
<i>Prosciurus magnus</i> †	X									X		
<i>Protosciurus mengi</i>	X									X		
<i>Scottimus ambiguus</i>	X					X						
<i>Scottimus exiguus</i> †	X								X			
<i>Willeumys viduus</i>	X		X	X	X							
<i>Wilsonemys planidens</i>	X								X			

locations, there appears to be a significant difference. Of the 14 rodent species identified from Obritsch Ranch in this study and the 19 rodent species previously identified from Fitterer Ranch (Korth et al. 2019), only eight are in common (Fig. 14).

Both *Eumys brachyodus* and *Ischyromys typus* are present in all sampling intervals at both locations. Perhaps the most significant difference between these assemblages is in the aplodontiids and sciurids. The Fitterer Ranch assemblage contains the aplodontiids *Altasciurus* and *Prosciurus*, whereas the only aplodontiid present at Obritsch Ranch is *Ninamys*. Similarly, the sciurid *Cedromus* is known from Fitterer Ranch but not at Obritsch Ranch, while *Oligospermophilus* is known from Obritsch Ranch

and not Fitterer Ranch. The only sciurid present at both localities is *Hesperopetes*; however, it should be noted that all the sciurids are relatively rare components of these assemblages, only represented by a few isolated teeth collected from screen washed sites.

The eomyids also vary between these locations. *Adjidaumo minimus* is present throughout the section at Fitterer Ranch and from sampling interval 2 at Obritsch Ranch. *Paradjidaumo trilophus* is also known from all sampling intervals at Fitterer Ranch, but it is limited to sampling interval 1 at Obritsch Ranch and is replaced by *Paradjidaumo obritschorum* in sampling intervals 2 and 3. *Adjidaumo minutus*, again, is present throughout the section at Fitterer Ranch but is completely absent at Obritsch Ranch.

TABLE 12. Local relative abundance of rodent families in well-described Whitneyan faunas. All values represent the percentage of specimens reported from a given fauna that are referred to each family. Abbreviations: BA, Blue Ash local fauna; CP, Cedar Pass local fauna; FRA, Fitterer Ranch Fauna A; FRB, Fitterer Ranch Fauna B; FRC, Fitterer Ranch Fauna C; ORB, Obritsch Ranch Fauna B; WH, White Hills local fauna.

Family	WH	FRA	FRB	FRC	ORB	CP	BA
Aplodontiidae	73	4	7	2	9	13	12
Castoridae	5	0	10	<1	1	9	<1
Cricetidae	7	54	57	9	18	16	59
Cylindrodontidae	1	0	0	0	0	0	0
Eomyidae	13	31	18	73	36	4	2
Eutypomyidae	0	0	0	0	0	1	<1
Florentiamyidae	0	0	1	0	0	32	17
Heliscomyidae	1	1	<1	15	32	0	<1
Heteromyidae	0	0	0	0	1	2	0
Ischyromyidae	0	6	6	<1	1	2	0
Sciuridae	0	3	1	1	3	22	9
Family indet.	0	0	0	0	0	<1	<1
Total Specimens	388	68	366	591	123	383	873

The species of *Heliscomys* present at each location are also distinct. *Heliscomys senex* and *H. borealis* are present at Fitterer Ranch (ranging from sampling intervals 5–6 and 2–6, respectively) and absent at Obritsch Ranch, while *H. cf. H. vetus* from sampling interval 2 at Obritsch Ranch is absent at Fitterer Ranch. The only species of *Heliscomys* in common to both localities is *H. medius*, which is known from the highest well-sampled interval at Fitterer Ranch (sampling interval 6) and the slightly younger sampling interval 2 at Obritsch Ranch (Fig. 14). In addition to the abundant species *Eumys brachyodus*, there are two other cricetid taxa reported from Fitterer Ranch (*Eumys lammersi* and *Willeumys viduus*) and one from Obritsch Ranch (*Scottimus* sp., cf. *S. ambiguus*). Though the cricetid taxon *Scottimus* was not reported from Fitterer Ranch by Korth et al. (2019), a single specimen (NDGS 4023: right dentary with i1 and m1–m3) recently collected from subunit 6B of Skinner (1951) at Fitterer Ranch (sampling interval 7) is referable to that genus, indicating that *Scottimus* is present at both locations with a local first appearance within subunit 6A or 6B of Skinner (1951).

Obritsch Ranch rodents compared to other Whitneyan rodent faunas.—To facilitate comparison to other well-described Whitneyan rodent faunas, the rodent assemblages from Fitterer Ranch and Obritsch Ranch were subdivided into discrete faunas based on stratigraphic position and similar taxonomic composition. This resulted in the recognition of three rodent faunas from Fitterer Ranch, with sampling intervals 1 and 2 combined into Fauna A, sampling intervals 4 and 5 combined into Fauna B, and

sampling interval 6 recognized as Fauna C. Sampling Intervals 3 and 7 were excluded because of the low diversity and small sample size from those intervals (Korth et al. 2019). At Obritsch Ranch, sampling intervals 2 and 3 were combined into a single fauna (Obritsch Ranch Fauna B) based on their close stratigraphic positions, with sampling interval 1 again excluded based on low diversity and sample size. This method resulted in the recognition of four stratigraphically stacked Whitneyan rodent faunas from North Dakota (though the oldest could be transitional Orellan/Whitneyan: Korth et al. 2019) for comparison to five well-described Whitneyan rodent faunas from elsewhere within the Great Plains region (Table 11). For seven of these nine faunas, specimen counts were available, allowing for comparison of relative abundance of rodent taxa between faunas (Table 12).

Obritsch Ranch Fauna B is most like Fitterer Ranch Fauna C, sharing six taxa in common (Table 11). Obritsch Ranch Fauna B shares four taxa in common with Fitterer Ranch Fauna A, Fitterer Ranch Fauna B, and the Blue Ash local fauna from southwestern South Dakota. However, the former two faunas largely share holdover Orellan taxa with Obritsch Ranch Fauna B while all taxa shared with the Blue Ash local fauna have Whitneyan first appearances (Table 11). Thus, the similarity of the former two faunas with Obritsch Ranch Fauna B may be influenced by biogeography, while the similarity to the Blue Ash local fauna may indicate those two faunas are similar in age (late Whitneyan). It is of note that Fitterer Ranch Fauna C shares the same four taxa in common with the Blue Ash local fauna and that no other Whitneyan rodent fauna

TABLE 13. Rodent diversity during the late Eocene and Oligocene in North America. Numbers include referrals of specimens at least to a specific genus, as well as inferred presence of taxa based on its presence in both younger and older faunas. Abbreviations: Ar, Arikareean; Ch, Chadronian; Du, Duchesnean; Or, Orellan; Wh, Whitneyan.

Family	Du	Ch	Or	Wh	Ar
Aplodontiidae	3	3	13	19	24
Castoridae	-	1	3	5	19
Cricetidae	1	2	9	17	16
Cylindrodontidae	8	12	2	2	1
Eomyidae	16	27	12	9	5
Eutypomyidae	5	3	2	1	1
Florentiamyidae	-	-	1	4	13
Geomyidae	1	1	2	2	30
Heliscomyidae	2	3	6	6	3
Heteromyidae	-	-	-	2	18
Ischyromyidae	16	11	6	2	-
Mylagaulidae	-	-	-	-	6
Pipestoneomyidae	2	1	-	-	-
Protoptychidae	1	-	-	-	-
Rodentia	3	5	3	2	2
Sciuravidae	2	2	-	-	-
Sciuridae	1	4	6	11	10
Simimyidae	2	1	-	-	-
Zapodidae	1	-	-	-	2
Zetamyidae	-	-	-	1	1
Taxa Present	64	76	65	83	151

includes more than two of those taxa (Table 11), indicating that Fitterer Ranch Fauna C may also be a late Whitneyan fauna.

Rodent diversity during the Whitneyan is dominated by aplodontiids and cricetids (Table 13); however, there is much variation in the relative diversity of rodent families

between faunas (Table 14). Additionally, local abundance within a given fauna does not always parallel local species diversity. In the White Hills local fauna of Montana, only a single species of aplodontiid is recognized, yet that species accounts for 73% of all rodent specimens collected from that fauna (Korth and Tabrum 2017). In the Cedar Pass \

TABLE 14. Relative diversity of rodent families in Whitneyan faunae. Abbreviations: BA, Blue Ash local fauna; CP, Cedar Pass local fauna; FRA, Fitterer Ranch Fauna A; FRB, Fitterer Ranch Fauna B; FRC, Fitterer Ranch Fauna C; ORB, Obritsch Ranch Fauna B; WH, White Hills local fauna.

Family	WH	FRA	FRB	FRC	ORB	CP	BA
Aplodontiidae	11	18	14	14	8	10	25
Castoridae	11	0	14	7	8	10	3
Cricetidae	22	18	21	14	15	30	23
Cylindrodontidae	11	0	0	0	0	0	0
Eomyidae	33	27	21	21	15	10	10
Eutypomyidae	0	0	0	0	0	5	3
Florentiamyidae	0	0	7	0	0	5	8
Heliscomyidae	11	9	7	21	15	0	5
Heteromyidae	0	0	0	0	8	5	0
Ischyromyidae	0	18	7	7	8	5	0
Sciuridae	0	9	7	14	23	15	23
Family indet.	0	0	0	0	0	5	3

local fauna of South Dakota, a single florentiamyid species is the most abundant rodent present, representing 32% of the specimens collected (Korth 2014). In the four North Dakota faunae, local abundance and local species diversity closely approximate each other (Table 12 versus Table 14). The main exception is the fact that sciurid diversity is relatively high (14–23%) in the Fitterer Ranch Fauna C and the Obritsch Ranch Fauna B, but local abundance of sciurids is low (1–3%). Similar trends are seen in the Blue Ash local fauna, where sciurids are one of the most diverse rodent families (nine species) and make up a small percentage of recovered specimens (9%) while three florentiamyid species account for 17% of rodent specimens (Korth, 2010b).

Patterns of local abundance of rodent species during the Whitneyan seem to be influenced in part by biogeography (Table 12). South Dakota faunae contain abundant specimens of cricetids, florentiamyids, sciurids, and aplodontiids. The two older North Dakota faunae are dominated by cricetids and eomyids while the two younger faunae are dominated by eomyids and heliscomyids. The White Hills local fauna is heavily dominated by aplodontiids, with eomyids making a secondary contribution. Some of these differences may result from the use of different specimen collection methods (e.g., surface collection versus screen washing), especially in cases where differences are related to relative body size. Differences in sampling methods may help explain the decrease in cricetid abundance in the younger two North Dakota faunae, where most collection was via screen washing while surface collecting (with a minor screen washing component) was employed in the two older North Dakota faunae.

The differential abundance of smaller-bodied taxa between these faunae is more difficult to attribute to

differences in sampling methods. All four North Dakota faunae and the White Hills local fauna were sampled at least in part via screen washing (Korth and Tabrum 2017; Korth et al. 2019; this study), while the two South Dakota faunae include substantial collection from anthills (Korth 2007, 2014), both of which tend to favor collection of isolated teeth from smaller-bodied taxa. Florentiamyid and heliscomyid species possessed teeth that are generally similar in size, as did the smaller species of eomyids (e.g., *Adjidaumo minimus*). Thus, the near lack of eomyids and heliscomyids in the South Dakota faunae despite the high abundance of florentiamyids is striking, as is the opposite pattern in the North Dakota faunae (Table 12). The White Hills local fauna differs as well in completely lacking florentiamyids and containing only a few heliscomyid specimens even though eomyids are the second most common rodent family (Korth and Tabrum 2017). Thus, there are some biogeographic influences on the local presence or absence and relative abundance of rodents at the family level during the Whitneyan. It is uncertain if this pattern is unique to the Whitneyan as few descriptions of late Eocene and Oligocene rodent faunae include specimen counts for all taxa, inhibiting detailed comparisons.

Whitneyan rodent biostratigraphy.—Compared to the preceding Orellan NALMA and the succeeding Arikarean NALMA, the Whitneyan NALMA has been more difficult to biostratigraphically define, resulting in fewer subdivisions (two versus four for both the Orellan and Arikarean: Prothero and Emry 2004). At the time of the most recent review of Whitneyan biostratigraphy (Prothero and Emry 2004), well-sampled and described rodent faunae were only known from the Slim Buttes area of northwestern South Dakota (Lillegraven 1970) and Harris Ranch

TABLE 15. Comparison of relative rates of origination, survival, and extinction of rodent species during the late Eocene through Oligocene in North America. Calculations of first (FADs) and last (LADs) appearances do not include taxa that uniquely occur within a single biozone. The retention category tracks the portion of the fauna that originated in an earlier biozone, while the survival category tracks the portion of the fauna that persists into the subsequent biozone. Abbreviations: FAD, first appearance datum; LAD, last appearance datum; NBU, species that are not biostratigraphically useful because they first appear in an older biozone and persist into a younger biozone.

NALMA	FADs	Unique	LADs	NBU	Retention	Survival
Duchesnean	19%	58%	19%	4%	23%	23%
Chadronian	18%	63%	15%	4%	19%	22%
Orellan	28%	46%	12%	14%	25%	42%
Whitneyan	20%	49%	30%	1%	31%	21%
Arikarean	12%	77%	11%	1%	12%	12%

in southwestern South Dakota (Simpson 1985). All other data on the Whitneyan rodent fauna came from scattered occurrences, resulting in many taxa being known only from a single locality (Prothero and Emry 2004). Since that time, stratigraphically constrained rodent faunae from South Dakota (Korth 2014), North Dakota (Korth et al. 2019; this study), and Montana (Korth and Tabrum 2017) have been described and the rodents of the Blue Ash local fauna from the upper portion of the section at Harris Ranch was revisited and further described (Korth 2010b). Those studies increase the number of well-sampled Whitneyan rodent faunae to nine (Table 11), and our knowledge of Whitneyan rodent diversity has increased from 14 taxa in 1994 (Korth 1994) to 83 today (Table 13: includes referrals to either the genus or species level). That increase provides a more extensive dataset for assessing Whitneyan rodent biostratigraphy and overall trends in rodent diversity during the Oligocene.

A total of 35 rodent species are now known only from Whitneyan faunae and another 14 species first appear in the Whitneyan and persist into later NALMAs (Table 11). Despite this increase in known Whitneyan rodent diversity, most species are known either from a single locality (28 species) or from a single geographic area (an additional 12 species), restricting their biostratigraphic utility. Only nine rodent species are known from multiple localities across different geographic areas, but many of those species still have restricted ranges. The castorid *Agnotocaster praetereadens*, the heliscomiid *Heliscomys medius*, and the sciurids *Hesperopetes blacki* and *Hesperopetes jamesi* are known from Whitneyan faunae in North Dakota and South Dakota. The aplodontiid *Campestrallomys siouxensis*, the cricetid *Scottimus lophatus*, and the florentiamiid *Kirkomys nebraskensis* are known from Whitneyan faunae in Nebraska and South Dakota. The eomyid *Lepodontomys douglassi* is known from Whitneyan faunae in Montana and South Dakota. Only one species, the cricetid *Eumys brachyodus*, is widely distributed, reported from Whitneyan faunae in Colorado, Montana, Nebraska,

North Dakota, South Dakota, and Saskatchewan (Galbreath, 1953; Korth, 1981, 2010b, 2014, 2018; Simpson, 1985; Storer, 1996; Korth and Tabrum, 2017; Korth et al., 2019). The only well-sampled Whitneyan fauna where *E. brachyodus* is not currently reported is unit F at the Slim Buttes (northwestern South Dakota), but that fauna does include *Eumys* sp. (Lillegraven 1970), so additional work on those specimens may reveal the presence of *E. brachyodus* in that fauna. Prior studies suggested that *E. brachyodus* was restricted to the late Whitneyan (e.g., Prothero and Whittlesey 1998; Prothero and Emry 2004), but it is now clear that *E. brachyodus* was present throughout the Whitneyan (Table 11). The broad geographic distribution of this species coupled with its typically high relative abundance within individual faunae clearly demonstrate that *E. brachyodus* is the most biostratigraphically useful rodent species for differentiating Orellan and Whitneyan rodent faunae.

Increased understanding of Whitneyan rodent diversity has also impacted the temporal distribution of many Orellan rodent taxa. Several taxa previously identified as last appearing in the latest Orellan (Prothero and Whittlesey 1998; Prothero and Emry 2004) are now known to persist into Whitneyan (*Adjidaumo*, *Ischyromys typus*, *Oligospermophilus*, *Paradjidaumo*, *Wilsoneumys*; Simpson 1985; Korth et al. 2019; this study) and younger faunae (*Eutypomys*, *Heliscomys*, *Prosciurus*, *Protosciurus*, *Tenudomys*; Storer 2002; Bailey 2004; Korth and Branciforte 2007). Overall, 22 of the 71 rodent species (31%) now recognized from Whitneyan faunae first appear in Orellan or older faunae, representing a 42% survivorship of rodent species across the Orellan/Whitneyan transition. That rate is far higher than observed at any other time in the late Eocene and Oligocene (Table 15). The Orellan rodent fauna is also unique in that 14% of species (8 out of 57) first appear in older faunae and have their last appearance in younger faunae, more than three times higher than observed in other late Eocene or Oligocene NALMAs (Table 15). Thus, Orellan and Whitneyan rodent faunae on average share

more taxa in common than rodent faunae from any other NALMA during the Paleogene, which helps explain prior difficulties in distinguishing Orellan and Whitneyan rodent faunae.

Trends in Oligocene rodent diversity.—At the end of the Eocene, Chadronian rodent faunae included a high diversity of eomyids, cylindrodontids, and ischyromyids (Table 13). The transition to Orellan rodent faunae in the early Oligocene is denoted by a marked decrease of all three of those families, though eomyid diversity remained comparatively high. At the same time, the diversity of heliscomyids doubled and aplodontiid and cricetid diversity more than quadrupled (Table 13). Florentiamyids made their first appearance in the Orellan, represented by *Ecclesimus tenuiceps* (Galbreath 1948; Korth 1989; Korth et al. 1991). Overall, Orellan rodent faunae were dominated by species of aplodontiids, eomyids, and cricetids.

The general composition of Whitneyan rodent faunae was similar to Orellan rodent faunae, with a few notable deviations. Aplodontiid and cricetid diversity continued to increase, eomyid and ischyromyid diversity continued to decline from their late Eocene peaks, and heliscomyid diversity remained steady. Heteromyids and zetamyids made their first appearances (Korth 2010b, 2014; Korth et al. 2019), while ischyromyids made their last appearance in the Whitneyan (e.g., Korth et al. 2019). A notable difference between Orellan and Whitneyan rodent faunae is an increase in sciurid diversity, a trend that was previously noted to begin in the Arikarean (Korth 1994). The transition from Whitneyan to Arikarean rodent faunae is marked by a substantial increase in overall diversity, from 83 to 151 currently recognized taxa, as well as a major shift in the relative diversity of rodent families. Aplodontiid, cricetid, and sciurid diversity remained stable or slightly increased, but the diversity of castorids, florentiamyids, geomyids, and heteromyids greatly increased (Table 13). The mylagaulids made their first appearance during the Arikarean, while the cylindrodontids and eutypomyids made their last appearances.

Our knowledge of Whitneyan rodents has greatly increased over the past decade. The application of screen washing and anthill collecting methods at Whitneyan localities, combined when possible with surface collection, facilitated the description of well-sampled faunae associated with detailed stratigraphic information. Those efforts resulted in the ability to make more accurate comparisons to rodent faunae from other NALMAs, improving our interpretation of trends in rodent evolution during the late Eocene and Oligocene in North America. Continued application of these methods, especially in highly fossiliferous areas such as the Big Badlands of southwestern South Dakota, will continue to improve our knowledge of rodent diversity, local abundance, and biogeographic distribution during this timeframe, allowing more detailed investigations of these topics to be undertaken in the future.

ACKNOWLEDGMENTS

We thank the Obritsch family for providing the NDGS with continued access to outcrops of the White River Group on their property over the past decades and the dozens of participants in the NDGS Public Fossil Digs Program that assisted in the discovery and collection of many of the specimens included in this study. T. Ford and P. Monaco spent many hours picking fossils out of the screen washed concentrate from sampling interval 2. J. Sullivan assisted in the sorting and measuring of specimens. The Department of Chemistry and Biochemistry at Nazareth College (Rochester, NY) provided lab space and equipment for this study.

LITERATURE CITED

- ALSTON, E.R. 1876. On the classification of the order Glires. Proceedings of the Zoological Society of London, 1876:61–98.
- BAILEY, B.E. 2004. Biostratigraphy and biochronology of early Arikarean through late Hemingfordian small mammal faunas from the Nebraska Panhandle and adjacent areas. *Paludicola* 4:81–113.
- BLACK, C.C. 1961. New rodents from the early Miocene deposits of Sixty-Six Mountain, Wyoming. *Breviora*, 146:1–7.
- . 1965. Fossil mammals from Montana. Part 2. Rodents from the early Oligocene Pipestone Springs local fauna. *Annals of Carnegie Museum*, 38:1–48.
- BOWDICH, T.E. 1821. An Analysis of the Natural Classifications of Mammalia for the Use of Students and Travellers. J. Smith, Paris, 115 pp.
- BRANDT, J.F. 1855. Beiträge zur nähern Kenntniss der Säugethiere Russlands. Kaiserlichen Akademie der Wissenschaften, Saint Petersburg, *Mémoires Mathématiques, Physiques et Naturelles*, 7:1–365.
- BURKE, J.J. 1934. New Duchesne River rodents and a preliminary survey of the Adjidaumidae. *Annals of Carnegie Museum*, 23:391–398.
- COPE, E.D. 1873a. Third notice of extinct Vertebrata from the Tertiary of the Plains. *Paleontological Bulletin*, 16:1–8.
- . 1873b. Synopsis of new Vertebrata from the Tertiary of Colorado, obtained during the summer of 1873. Washington, Government Printing Office, October 1873, pp. 1–19.
- EMRY, R.J., AND W.W. KORTH. 2007. A new genus of squirrel (Rodentia, Sciuridae) from the mid-Cenozoic of North America. *Journal of Vertebrate Paleontology*, 27:693–698.
- FISCHER DE WALDHEIM, G. 1817. *Adversaria zoologica*. *Mémoires del la Société Impériale des Naturalistes du Moscou*, 5:357–428.
- FLYNN, L.J., E.H. LINDSAY, AND R.A. MARTIN. 2008. Geomorpha. Pp. 428–455, in *Evolution of Tertiary Mammals of North America, Volume 2: Small Mammals, Xenarthrans, and Marine Mammals* (C.M. Janis, G.R. Gunnell and M.D. Uhen, eds.). Cambridge University Press, Cambridge.
- GALBREATH, E.C. 1948. An additional specimen of the rodent *Dikkomya* from the Miocene of Nebraska. *Transactions of the Kansas Academy of Sciences*, 51:316–317.
- . 1953. A contribution to the Tertiary geology and paleontology of northeastern Colorado. *University of Kansas Paleontological Contributions, Vertebrata*, 13:1–120.
- GRAY, J.E. 1868. Synopsis of the species of Saccomyinae, or pouched mice, in the collection of the British Museum. *Proceedings of the Zoological Society of London*, 1868:199–206.
- HAY, O.P. 1930. Second bibliography and catalog of the fossil vertebrates of North America. *Carnegie Institute of Washington Publication*, 390:1–1074.
- HEATON, T.H. 1996. Ischyromyidae. Pp. 373–398, in *The Terrestrial Eocene-Oligocene Transition in North America* (D.R. Prothero and R.J. Emry, eds.). Cambridge University Press, New York.
- HEMPRICH, W. 1820. *Grundriss der Naturgeschichte für höhere Lehranstalten Entworfen von Dr. W. Hemprich*. August Rucher, Berlin; Friedrich Volke, Vienna.
- JANIS, C.M., G.F. GUNNELL, AND M.D. UHEN (EDS.). 2008. *Evolution of Tertiary Mammals of North America, Volume 2: Small Mammals*,

- Xenarthrans, and Marine Mammals. Cambridge University Press, Cambridge.
- KELLY, T.S. 1992. New Uintan and Duchesnean (middle and late Eocene) rodents from the Sespe Formation, Simi Valley, California. *Southern California Academy of Sciences Bulletin*, 91:97–120.
- . 2010. New records of Rodentia from the Duchesnean (middle Eocene) Simi Valley landfill local fauna, Sespe Formation, California. *Paludicola*, 8:49–73.
- KORTH, W.W. 1980. *Paradjidaumo* (Eomyidae, Rodentia) from the Brule Formation, Nebraska. *Journal of Paleontology*, 54:993–941.
- . 1981. New Oligocene rodents from western North America. *Annals of Carnegie Museum*, 50:289–318.
- . 1987. Sciurid rodents (Mammalia) from the Chadronian and Orellan (Oligocene) of Nebraska. *Journal of Paleontology*, 61:1247–1255.
- . 1989. Aplodontid rodents (Mammalia) from the Oligocene (Orellan and Whitneyan) Brule Formation, Nebraska. *Journal of Vertebrate Paleontology*, 9:400–414.
- . 1994. *The Tertiary Record of Rodents in North America*. Plenum Press, New York.
- . 1995. Skull and upper dentition of *Heliscomys senex* Wood (Heliscomyidae: Rodentia). *Journal of Paleontology*, 69:191–194.
- . 1998. A new beaver (Rodentia, Castoridae) from the Orellan (Oligocene) of North Dakota. *Paludicola*, 1:127–131.
- . 2007. Mammals from the Blue Ash local fauna (late Oligocene), South Dakota. *Rodentia, Part 1: Families Eutyromyidae, Eomyidae, Heliscomyidae, and Zetamys*. *Paludicola*, 6:31–40.
- . 2008. Generic allocation and probable horizon of occurrence of the enigmatic geomyoid rodent *Diplolophus parvus* Troxell from northeastern Colorado. *Paludicola*, 6:139–143.
- . 2010a. Mammals from the Blue Ash local fauna (late Oligocene), South Dakota. *Rodentia, Part 5: Family Cricetidae*. *Paludicola*, 7:117–136.
- . 2010b. Mammals from the Blue Ash local fauna (late Oligocene), South Dakota. *Rodentia, Part 6: Family Castoridae and additional Eomyidae with a summary of the complete rodent fauna*. *Paludicola*, 8:8–13.
- . 2013. Review of *Paradjidaumo* Burke (Rodentia, Eomyidae) from the Eocene and Oligocene (Duchesnean-Whitneyan) of North America. *Paludicola*, 9:111–126.
- . 2014. Rodents (Mammalia) from the Whitneyan (middle Oligocene) Cedar Pass fauna of South Dakota. *Annals of Carnegie Museum*, 82:373–397.
- . 2018. Oligocene (Orellan-Whitneyan) cricetid rodents (Mammalia, Rodentia) from Sioux County, Nebraska. *Paludicola*, 12:1–12.
- . 2019. Rodents (Mammalia) from the early Oligocene (Orellan) Cook Ranch local fauna of southwestern Montana. *Annals of Carnegie Museum*, 85:91–111.
- KORTH, W.W., AND C. BRANCIFORTE. 2007. Geomyoid rodents (Mammalia) from the Ridgeview local fauna, early-early Arikarean (late Oligocene) of western Nebraska. *Annals of Carnegie Museum*, 76:177–201.
- KORTH, W.W., AND R.J. EMBRY. 1991. The skull of *Cedromus* and a review of the Cedromurinae (Rodentia, Sciuridae). *Journal of Paleontology*, 65:986–994.
- KORTH, W.W., R.J. EMBRY, C.A. BOYD, AND J.J. PERSON. 2019. Rodents (Mammalia) from Fitterer Ranch, Brule Formation (Oligocene), North Dakota. *Smithsonian Contributions to Paleobiology*, 103:1–45.
- KORTH, W.W., R.J. EMBRY, AND M.R. MUSSO. 2015. Systematics, cranial morphology, and taphonomy of the eomyid rodent *Adjidaumo minimus* (Matthew, 1903) from the Chadronian (late Eocene), Flagstaff Rim area, Wyoming. *Journal of Vertebrate Paleontology*, doi: 10.1080/02724634.2014.1001854 (11 pages)
- KORTH, W.W., AND A.R. TABRUM. 2017. A unique rodent fauna from the Whitneyan (middle Oligocene) of southwestern Montana. *Annals of Carnegie Museum*, 84:319–340.
- KORTH, W.W., J.H. WAHLERT, AND R.J. EMBRY. 1991. A new species of *Heliscomys* and recognition of the family Heliscomyidae (Geomyoidea, Rodentia). *Journal of Vertebrate Paleontology*, 11:247–256.
- LEIDY, J. 1856. Notices of remains of extinct Mammalia discovered by Dr. F.V. Hayden in Nebraska Territory. *Proceedings of the Academy of Natural Sciences of Philadelphia*, 8:88–90.
- LILLEGRAVEN, J.A. 1970. Stratigraphy, structure, and vertebrate fossils of the Oligocene Brule Formation, Slim Buttes, northwestern South Dakota. *Geological Society America Bulletin*, 81:831–850.
- MACDONALD, J.R. 1963. The Miocene faunas from the Wounded Knee area of western South Dakota. *Bulletin of the American Museum of Natural History*, 125:139–238.
- MATTHEW, W.D. 1903. The fauna of the *Titanotherium* beds at Pipestone Springs, Montana. *Bulletin of the American Museum of Natural History*, 16:1–19.
- MURPHY, E.C., J.W. HOGANSON, AND N.F. FORSMAN. 1993. The Chadron, Brule and Arikaree formations in North Dakota. The buttes of southwestern North Dakota. Report of Investigations Number 96 North Dakota Geological Survey.
- OGG, J.G. 2012. Geomagnetic polarity time scale. Pp. 85–114, in *The Geologic Timescale 2012* (F. M. Gradstein, J. G. Ogg, M. D. Schmitz, and G. M. Ogg, eds.). Elsevier, Oxford.
- PROTHERO, D.R. 1996. Magnetic stratigraphy of the White River Group in the High Plains. Pp. 262–277, in *The Terrestrial Eocene-Oligocene Transition in North America* (D.R. Prothero and R.J. Emry, eds.). Cambridge University Press, New York.
- PROTHERO, D.R., AND R.J. EMBRY. 2004. The Chadronian, Orellan, and Whitneyan North American Land Mammal Ages. Pp. 156–168, in *Late Cretaceous and Cenozoic Mammals of North America: Biostratigraphy and Geochronology* (M.O. Woodburne, ed.). Columbia University Press, New York.
- PROTHERO, D.R., AND K.E. WHITTLESEY. 1998. Magnetic stratigraphy and biostratigraphy of the Orellan and Whitneyan land-mammal “ages” in the White River Group. *Geological Society of America Special Papers*, 325:39–61.
- RENSBERGER J.M. 1975. *Haplomys* and its bearing on the origin of the aplodontoid rodents. *Journal of Mammalogy*, 56:1–14.
- RUSSELL, L.S. 1954. Mammalian fauna of the Kishenehn Formation, southeastern British Columbia. *Bulletin of the National Museum of Canada*, 132:92–111.
- SIMPSON, G.G. 1945. The principles of classification and a classification of mammals. *Bulletin of the American Museum of Natural History*, 85:1–350.
- SIMPSON, W.F. 1985. Geology and paleontology of the Oligocene Harris Ranch Badlands, southwestern South Dakota. *Dakoterra*, 2:303–333.
- SKINNER, M.F. 1951. The Oligocene of western North Dakota. Pp. 51–58, in *Society of Vertebrate Paleontology Guidebook, 5th Annual Field Conference, Western South Dakota, August – September 1951* (J. D. Bump, ed.).
- STIRTON, R.A. 1935. A review of the Tertiary beavers. University of California Publications in Geological Sciences, 23:391–458.
- STONE, W.J. 1973. Stratigraphy and sedimentary history of middle Cenozoic (Oligocene and Miocene) deposits in North Dakota. Unpublished Ph.D. dissertation, University of North Dakota, Grand Forks, 217 pp.
- STORER, J.E. 1996. Eocene-Oligocene faunas of the Cypress Hills Formation, Saskatchewan. Pp. 240–261, in *The Terrestrial Eocene-Oligocene transition in North America* (D.R. Prothero and R.J. Emry, eds.). Cambridge University Press, New York.
- . 2002. Small mammals of the Kealey Springs local fauna (early Arikarean; late Oligocene) of Saskatchewan. *Paludicola* 3:105–133.
- TABRUM, A.R., D.R. PROTHERO, AND D. GARCIA. 1996. Magnetostratigraphy and biostratigraphy of the Eocene–Oligocene transition, southwestern Montana. Pp. 278–311, in *The Terrestrial Eocene–Oligocene Transition in North America* (D.R. Prothero and R.J. Emry, eds.) Cambridge University Press, New York.
- TEDFORD, R.H., L.B. ALBRIGHT III, A.D. BARNOSKY, I. FERRUSQUIA-

- VILLAFRANCA, R.M. HUNT, JR., J.E. STORER, C.C. SWISHER III, M.R. VOORHIES, S.D. WEBB, AND D.P. WHISTLER. 2004. Mammalian biochronology of the Arikareean through Hemphillian interval (late Oligocene through early Pliocene Epochs). Pp. 169–231, in *Late Cretaceous and Cenozoic Mammals of North America: Biostratigraphy and Geochronology* (M.O. Woodburne, ed.). Columbia University Press, New York.
- VIANEY-LIAUDE, M., H.G. GOMES, AND L. MARIVAUX. 2013. Early adaptive radiations of Aplodontoidea (Rodentia, Mammalia) on the Holarctic region: systematics, and phylogenetic and paleobiogeographic implications. *Paläontologische Zeitschrift*, 87:83–120.
- WAHLERT, J.H. 1984. *Kirkomys*, a new florentiamyid (Rodentia, Geomyoidea) from the Whitneyan of Sioux County, Nebraska. *American Museum Novitates*, 2793:1–8.
- . 1991. The Harrymyinae, a new heteromyid subfamily (Rodentia, Geomorpha), based on cranial and dental morphology of *Harrymys* Munthe, 1988. *American Museum Novitates*, 3013:1–23.
- WILSON, R.W. 1949. Early Tertiary rodents of North America. *Contribution to Paleontology*, Carnegie Institution of Washington Publication, 584:71–164.
- WINGE, A.H. 1887. Jordfundne og nulevende Gnavere (Rodentia) fra Lagoa, Minas Geraes, Brasilien. *Universitet Museo Lundil*, Copenhagen, 1:1–300.
- WOOD, A.E. 1935. Evolution and relationships of the heteromyid rodents with new forms from the Tertiary of western North America. *Annals of Carnegie Museum*, 24:73–262.
- . 1937. The mammalian fauna of the White River Oligocene, Part 2, Rodentia. *Transactions of the American Philosophical Society*, 28:155–269.
- WOOD, A.E., AND R.W. WILSON. 1936. A suggested nomenclature for the cusps of the cheek teeth of rodents. *Journal of Paleontology*, 10:388–391.